

MicroMAPS Team
Spring 2005 Final Report
AOE 4065

Team Members

Ludovic Burton
Brian Gardner
Liam Flemming

Arthur Jarjisian
Leslie Johnson
Tyler McCall
David Simon



The Altair¹

AEROSPACE AND OCEAN ENGINEERING DEPARTMENT
VIRGINIA POLYTECHNIC INSTITUTE AND STATE UNIVERSITY
BLACKSBURG, VIRGINIA

MAY 5, 2005

Table of Contents

LIST OF FIGURES	3
LIST OF TABLES	4
ABSTRACT	5
I INTRODUCTION	6
I - A PROJECT OBJECTIVE	6
I - B SUMMARY OF FALL 2004	6
I - C SUMMARY OF SPRING 2005	7
I - D HISTORY OF MICROMAPS	8
I - E ENGINEERING OBJECTIVE	9
I - F SCIENCE MISSION	9
I - G HOW IT WORKS	10
II UAV SELECTION	12
II - A UAV RECOMMENDATION	12
II - B RISK ASSESSMENT	15
III THE ALTAIR	18
III - A THE ALTAIR	18
III - B ALTAIR CONTROL OPERATIONS	19
III - C PAYLOAD INSTALLATION	21
IV PAYLOAD	22
IV - A PAYLOAD OVERVIEW	22
IV - B INTERNAL PAYLOAD	22
IV - C EXTERNAL PAYLOAD	23
IV - D PAYLOAD WEIGHT	24
IV - E EMERGENCY RECOVERY PARACHUTE	25
V PRESSURE VESSEL	27
V - A DESIGN OF THE PRESSURE VESSEL	27
V - B PRESSURE VESSEL MATERIAL	29
V - C PRESSURE VESSEL SHAPE AND THICKNESS	30
V - D PRESSURE CONNECTORS	37
V - E PRESSURE VALVES	38
V - F GASKET DESIGN	38
VI THERMAL MANAGEMENT	39
VI - A TEMPERATURE REQUIREMENTS	39
VI - B THERMAL MODEL DESCRIPTION	42
VI - C TEMPERATURE ANALYSIS	45
VI - D THERMO-ELECTRIC COOLING ASSEMBLY	51
VII DATA ACQUISITION SYSTEM AND POWER SUPPLY SYSTEM	65
VII - A PAYLOAD DATA ACQUISITION RATE	66
VII - B CURRENT SETUP/INDEPENDENT METHOD	66
VII - C ALTAIR DATA COLLECTION	67
VII - D PAYLOAD BAY CHARACTERISTICS	68
VII - E DATA ACQUISITION WITH THE ALTAIR	69
VIII APPENDIX	73
VIII - A DIFFERENT COOLING SYSTEMS	73
REFERENCES	80

List of Figures

FIGURE 1 - MICROMAPS INSTRUMENT	10
FIGURE 2 - SCHEMATIC OF A GFCR	11
FIGURE 3 - CLASS A MISHAPS PER 100,000 FLIGHT HOURS	16
FIGURE 4 - CAUSES OF UAV CLASS A MISHAPS	17
FIGURE 5 - THE ALTAIR.....	18
FIGURE 6 - EXTERNAL POD MOUNTING LOCATIONS.....	19
FIGURE 7 - C-BAND DATALINK ARCHITECTURE	20
FIGURE 8 - KU-BAND DATALINK ARCHITECTURE.....	20
FIGURE 10 - PRESSURE VESSEL MOUNTED IN THE ALTAIR PAYLOAD BAY	23
FIGURE 11 - EXTERNAL POD CONCEPT FROM SARGENT FLETCHER INC.	24
FIGURE 13 - MICROMAPS, POWER SUPPLY, AND COMPUTER ON PRESSURE VESSEL BASE PLATE.....	29
FIGURE 14 - SHEAR FORCE AND BENDING MOMENT OF A 19 INCH BEAM WITH CLAMPED ENDS.....	33
FIGURE 15 - BASE PLATE STRESS DISTRIBUTION AT 15 PSI	34
FIGURE 16 - PRESSURE VESSEL STRESS DISTRIBUTION AT 15 PSI.....	35
FIGURE 17 - STRESS ANALYSIS MESH	35
FIGURE 18 - FISCHER CO. PRESSURE CONNECTOR (EXAMPLE).....	37
FIGURE 20 - TEMPERATURE VARIATION IN THE ALTAIR PAYLOAD BAY	40
FIGURE 21 - MODEL USED FOR THERMAL ANALYSIS	43
FIGURE 22 - NATURAL CONVECTION.....	45
FIGURE 23 - CAD MODEL USED FOR THERMAL ANALYSIS, SOME PARTS OMITTED	46
FIGURE 24 - TEMPERATURE VARIATION WITHOUT COOLING	47
FIGURE 25 - RATE OF TEMPERATURE CHANGE INSIDE PRESSURE VESSEL WITHOUT COOLING.....	48
FIGURE 26 - BASE PLATE TEMPERATURE VARIATION (°C) WITHOUT COOLING.	50
FIGURE 27 - TYPICAL THERMOELECTRIC COOLING ASSEMBLY.....	51
FIGURE 28 - THERMOELECTRIC COOLING ASSEMBLY, CP-218	53
FIGURE 29 - DIMENSIONED CP-218 THERMOELECTRIC COOLING ASSEMBLY.....	54
FIGURE 30 - TC-24-25-RS232 TEMPERATURE CONTROLLER.....	55
FIGURE 31 - DIMENSIONED TC-24-25-RS232 TEMPERATURE CONTROLLER	55
FIGURE 32 - ASTRODYNE SD-350 SERIES 350 WATT SINGLE OUTPUT DC/DC CONVERTER.....	57
FIGURE 33 - SCHEMATIC OF THE ASTRODYNE SD-350 SERIES SINGLE OUTPUT DC/DC CONVERTER.....	57
FIGURE 34 - SPECIFICATIONS OF THE ASTRODYNE SD-350 SERIES SINGLE OUTPUT DC/DC CONVERTER.....	58
FIGURE 35 - TEMPERATURE VARIATION WITH TWO 218 WATT COOLERS	59
FIGURE 36 - MICROMAPS INSTRUMENT TEMPERATURE VARIATION DURING FLIGHT (SIMULATION).....	60
FIGURE 37 - HEAT REMOVAL REQUIRED AND CORRESPONDING TEMPERATURE VERSUS TIME	60
FIGURE 38 - RATE OF TEMPERATURE VARIATION VERSUS TIME.....	61
FIGURE 39 - TEMPERATURE VARIATION OF MICROMAPS FOR AN INITIAL SYSTEM TEMPERATURE OF 15°C .	62
FIGURE 40 - BASE PLATE TEMPERATURE WITH TIME AND HEAT PROPAGATION DURING COOLING PROCESS. .	63
FIGURE 41 - ALTAIR DEPLOYMENT	68
FIGURE 42 - ALTAIR PAYLOAD BAY CHARACTERISTICS	69
FIGURE 43 - PAYLOAD DATA CABLE INTERFACE	71
FIGURE 39 - DESCRIPTION OF THE FUNCTIONING OF A HEAT PIPE.	75
FIGURE 40 - PHOTOGRAPH OF A TUBED FLOW COLD PLATE MANUFACTURED BY LYTRON¹⁶.	77
FIGURE 41 - REPRESENTATION OF A DISTRIBUTED FLOW COLD PLATE.	77

List of Tables

TABLE 1 - POSSIBLE UAVS	14
TABLE 3 - APPROXIMATE PAYLOAD TABLE OF WEIGHTS.....	24
TABLE 4 - PHYSICAL PROPERTIES OF ALUMINUM ALLOY 2014 AND 6061	30
TABLE 5 - PRESSURE VESSEL MINIMUM REQUIRED WALL THICKNESS ESTIMATE.....	31
TABLE 6 - FEA ANALYSIS SUMMARY	36
TABLE 7 - PROPERTIES OF ALUMINUM ALLOYS	42
TABLE 8 - CONTROLLER SPECIFICATIONS	56
TABLE 9 - COST ANALYSIS.....	ERROR! BOOKMARK NOT DEFINED.

Abstract

This report presents the 2004-2005 MicroMAPS design team's solution to modify an Unmanned Aerial Vehicle (UAV) to accommodate MicroMAPS, which measures carbon monoxide in the atmosphere. This paper covers a brief background of the instrument, the UAV selection process, and major design considerations including packaging, internal pod environment control and data acquisition.

After research and analysis of the different UAVs available to NASA, the Altair was chosen for this project because it has the best combination of altitude and endurance performance characteristics. In addition, the Altair has the capability to carry an internal or external payload.

It was decided to encase MicroMAPS and its supporting components inside a temperature-regulated rectangular pressure vessel for installation in the Altair. The entire package will be modular for ease of transfer between different UAV platforms.

MicroMAPS, along with the other components (computer and power supply), will be attached to an aluminum plate and covered by a welded aluminum case with a viewing window for the sensor, and pressure connectors for power and data transfer. The vessel will be sealed with a gasket to maintain atmospheric pressure to prevent condensation inside the package. Because MicroMAPS is sensitive to temperature variations while taking data, the internal temperature will be controlled using two thermoelectric coolers attached to the outside of the base plate.

Two data acquisition methods are available. The experimenters can choose the method they desire: either use the Altair's communications system to transfer experimental data in real time, or store the data inside the package for transfer after the UAV is on the ground.

I Introduction

I - A Project Objective

The objective of the 2004-2005 MicroMAPS team was to place the MicroMAPS instrument on a UAV platform. This includes first choosing a UAV that satisfies various scientific requirements such as time of flight, ceiling and availability, given by NASA. The second part of the analysis, and the focus of this report, details the installation, control and monitoring of the payload in the UAV. The importance of modularity in the payloads of UAVs was not overlooked. The culmination of this project is to provide NASA Langley with detailed plans for implementation of MicroMAPS on a UAV platform.

I - B Summary of Fall 2004

Previously, after reviewing a number of possible UAVs, the team recommended the Altus and the Altair manufactured by General Atomics. The focus of this report is the modification of the Altair to accommodate the MicroMAPS package.

A pressure vessel will be used to prevent water condensation on the MicroMAPS instrument as well as the data acquisition computer and power supply to the package. The entire MicroMAPS package, computer and power supply will be contained in this vessel.

Potential cooling systems were selected to help cool the pressure vessel while the aircraft is on the ground. This is to ensure that the MicroMAPS package will not over heat while on the ground and will be stabilized once the aircraft reaches altitude.

The payload thus consists of the pressure vessel, computer, power supply and cooling system. The team examined methods of mounting the pressure vessel in the

internal payload bay of the Altair and recommended, as an alternative, an external payload configuration that could be more easily transferred to alternate platforms.

Lastly, the team recommended two possible methods for data acquisition from the MicroMAPS package while onboard the Altair. One method uses a system built into the pressure vessel while the other relies on the Altair's data transfer communications equipment.

I - C Summary of Spring 2005

In the Spring 2005 semester, the team performed a more detailed analysis of the pressure vessel, cooling system, and external payload. The team also determined how to provide power to and control the cooling system. Detailed CAD drawings were made of all the components to enable NASA to build and install the complete pressure vessel into the Altair based on the final report.

This phase of the report addresses four major issues relating to the pressure vessel. The first is the design of a seal to maintain pressure using a gasket. Secondly, stress and fatigue analyses were performed to obtain the optimum aluminum thickness. Thirdly, a valve to fill the vessel was selected and pressure connectors were chosen. Lastly, detailed CAD drawings of the final design were produced to assist in the manufacturing process.

A detailed thermal analysis was performed to determine the required size of the thermoelectric coolers needed to cool the vessel under various outside temperature conditions and time constraints.

Detailed CAD drawings show how all the components will be bolted to the internal payload bay of the Altair as well as a potential external bay. These CAD

drawings also show how the Altair's airframe skin must be modified to allow the instrument to view the atmosphere below. Finally, the total weight was determined, and structural analysis was performed to verify an acceptable factor of safety.

I - D History of MicroMAPS

The development of MicroMAPS originally stemmed from the MAPS (Measurement of Air Pollution from Satellites) instrument. MAPS was originally flown on the Space Shuttle on STS 2 in November 1981. It was also flown again in October of 1984 and April and October of 1994.

After successful use of the MAPS instrument, MicroMAPS was developed as part of the Small Spacecraft Technology Initiative (SSTI). The major goals for SSTI were: to demonstrate how to reduce the cost and development time of space missions for science and commercial applications; to demonstrate new design and qualification methods for small spacecraft, including use of commercial and performance-based specifications and integration of small instrumentation technology into bus design; and to proactively promote commercial technology applications. Two spacecraft, Lewis and Clark, were developed as part of this program; MicroMAPS was built for the Clark spacecraft. However, the SSTI program was terminated in February of 1998 because of mission costs and delays and MicroMAPS was not flown.

In the summer of 2004, MicroMAPS flights began on the Proteus high-altitude research vehicle as part of a Virginia Space Grant Consortium (VSGC) project involving students from Old Dominion University, Virginia Tech, and the University of Virginia. The Proteus aircraft, designed by Scaled Composites LLC, was flown by Mike Melvill, Vice President of Scaled Composites and the first person to fly a commercial vehicle into

space (Space Ship One). Flights on Proteus continued from July through September of 2004.

I - E Engineering Objective

The engineering objective of the MicroMAPS instrument was to develop a small, low-cost apparatus to complete the same task of monitoring the atmosphere on a global scale as an already existing larger and more expensive instrument (MAPS).

I - F Science Mission

The primary goal of the MicroMAPS system is to study tropospheric activity using remote sensing. The instrument monitors carbon monoxide in the troposphere in order to understand sources, sinks, transport and distribution of the gas. Pollution concentration and density can also be monitored and three-dimensional models of the gas distribution can be generated. The MicroMAPS system is also capable of tracking the movement of the air pollution in the atmosphere by monitoring the changes in intensity and location over an extended period of time. MicroMAPS can monitor a specific region in the atmosphere to generate data for gap regions of previously generated data and can also monitor regions previously monitored to verify existing data.

The science goal of the MicroMAPS system is to provide knowledge of chemical activity in the atmosphere over the entire earth. This knowledge will help develop a better understanding of how climate is affected by the chemical composition of the atmosphere. A picture of the instrument is shown in Figure 1.

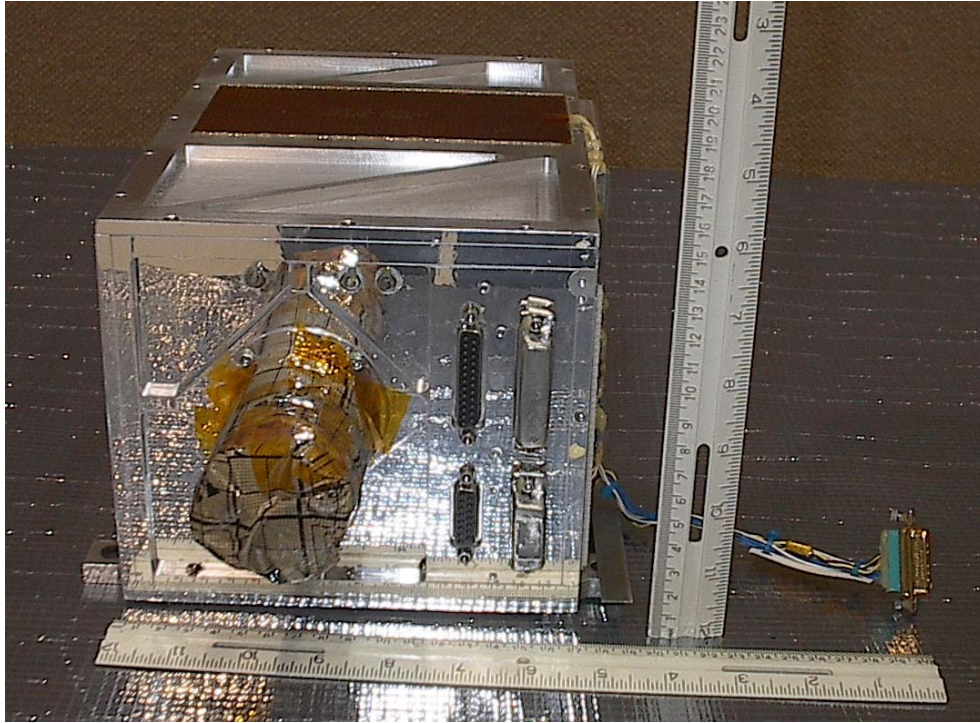


Figure 1 - MicroMAPS Instrument

I - G How it Works²

The MicroMAPS instrument is a nadir-viewing gas filter correlation radiometer (GFCR). A schematic of the optical path is shown in Figure 2. The system observes the area directly underneath itself, operating in the 4.67-micrometer band of the electromagnetic spectrum, which is ideal for observing carbon monoxide. This GFCR is an opto-electric path switching sensor capable of detecting airborne pollutants such as carbon monoxide, methane and nitrogen oxides. The device uses a polarization modulator in conjunction with a beam splitter to allow for rapid optical-path switching without the use of moving parts. Solar energy reflected by the gasses in the atmosphere is band-limited and polarized. As the light enters the instrument through the viewing window, the light radiation passes through a polarization-sensitive beam splitter and is alternated between two optical paths. One component of the polarized photons is guided through a

vacuum cell while the other is sent through a correlation cell containing the gas, which the sensor is calibrated to detect. The gas in the correlation cell acts as a filter and the radiation signal is thus altered. When the target gas is present in the atmospheric path, the atmosphere introduces a spectral content into the incoming solar energy signal which is correlated with the absorption line spectrum of the gas cell, causing the magnitude of the output signal to be altered. After the radiation from the two paths is recombined, an analysis of the difference in signal strengths will show the amount of target gas present in the line of sight of the instrument.

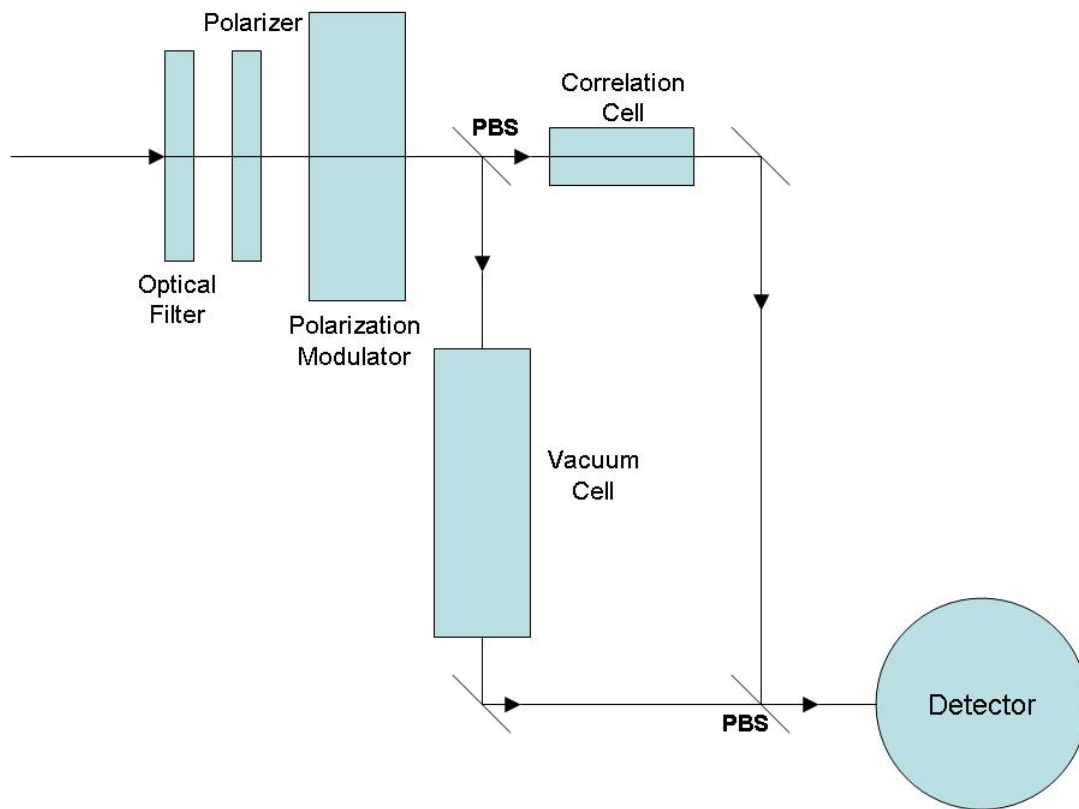


Figure 2 - Schematic of a GFCR

II UAV Selection

II - A UAV Recommendation

In selecting the UAV best suited to the requirements of the MicroMAPS package, several different options were examined and evaluated based on the following pre-determined criteria. The original project requirements, recommended by NASA, to enable accurate data collection specified that the UAV should have a cruise altitude of 60,000 ft. minimum and also have an endurance of at least 36 hours. Table 1 shows the different options examined for this project and the specifications of each. Another restriction in the selection of an aircraft is the limited number of options found at NASA Dryden.

The four UAVs that are available from NASA are the Altair, Altus, Altus 2, and Perseus B. A compromise needed to be made on the altitude or the endurance because none of the vehicles met both requirements. If the cruise altitude criterion was to be met, Altus, Altus 2 or Perseus B should be chosen. On the other hand if the endurance criterion was to be met, Altair should be the UAV selected. Thus, Table 1 shows that none of those UAVs meet both of the criteria. We were informed by NASA scientists that for the MicroMAPS system to function properly, it must be at high altitude and that an endurance of approximately 24 hours would suffice. Because of this determination, the endurance requirement was relaxed. Therefore, the UAV that would best accommodate the MicroMAPS package is the Altus because it has the longest endurance for a UAV with cruise altitude over 60,000 ft.

Another requirement of this project is that it should be possible to easily remove and reinstall the package. Upon further research, it was found that the Perseus B,

though not in NASA possession at the moment, has a detachable cargo section. This would make the exchange of cargo packages most efficient.³ Although the Perseus B has an endurance of seven hours at 60,000 ft, the production model of this aircraft will have a 24 hour endurance which would match the relaxed endurance requirement. Therefore the production Perseus B, pending NASA's acquisition of it, would also be very well suited to accommodate the MicroMAPS package.

The Helios UAV, manufactured by Aerovironment JPL, was also examined to determine if it is a suitable option to carry the MicroMAPS system. The maximum altitude for Helios is above 90,000 feet and the target endurance is 96 hours at 50,000 to 70,000 feet.⁴ The solar panels which power the 14 brushless electric motors are 19% efficient and are required to power all of the motors in addition to charging the lithium battery backup system.⁵ This means that there is little power available for MicroMAPS, the computer and cooling system. In addition to lack of auxiliary power, there is a high risk associated with using an untested system. There have been two Helios prototypes, one of which was lost during testing. This survival rate is unacceptable for the MicroMAPS instrument, and therefore the Helios was not considered.

Table 1 - Possible UAVs⁶

	General Atomics					
	Altair	Altus	I-Gnat	Mariner	Predator	Predator B
Cruise altitude(ft)	52,000	65,000	20,000	52,000	25,000	50,000
Endurance(hrs)	32-36	30	42	49	29	30
Cruise speed(mph)	140-150	258	140	253	80	220
Payload weight(lb)	660-700 internal	330	650	Int.- 800	450	Int.- 800
Payload size(cu. in)	n/a	n/a	n/a	n/a	n/a	n/a
Power plant Thrust and Weight	700hp Honeywell TPE 331-10 @ 300lb	100 hp Rotax 912-2T	100hp Rotax 914	Honeywell TPE 331-10T	100 hp Rotax 914	n/a
Fuel weight(lb)	3,000	614	n/a	6,000	665	3,000
Weight(lb)	-----	-----	-----	-----	-----	-----
Empty weight(lb)	3,250	1,186	850	10,500	1130	2,650
Wingspan(ft)	86	55.3	42	86	48.7	66
Length(ft)	36	23.6	21	36	27	36
	Aurora Flight Sciences		Boeing	Northrop Grumman	Scaled Composites	
	Theseus	Perseus	X-45	Global Hawk	Raptor	
Cruise altitude(ft)	35,000-60,000	65,620	40,000	50,000-60,000	65,000	
Endurance(hrs)	36	8-24(Aurora)	n/a	42	8	
Cruise speed(mph)	n/a	112	M 0.8	397	n/a	
Payload weight(lb)	1,800	330(nose)	1,500	n/a	75	
Payload size(cu. in)	21.6x21.6x74	21.6x21.6x74	n/a	n/a	n/a	
Power plant Thrust and Weight	n/a	n/a	6300 lb thrust Honeywell F124	8294 lb thrust Rolls-Royce AE3007H	100hp Two stage Rotax	
Fuel weight(lb)	n/a	n/a	2,960	14,500	n/a	
Weight(lb)	5,511	2,200	-----	-----	-----	
Empty weight(lb)	n/a	n/a	8,000	n/a	n/a	
Wingspan(ft)	117	71.5	34	116.2	66	
Length(ft)	29.2	26.7	27	44.4	24.4	

II - B Risk Assessment

There is an inherent risk in flying a scientific package on a UAV because of reliability concerns. Figure 3 shows the mishap rate of three UAV models since 1994. Because the Altair is a modified Predator, the data for the RQ-1/Predator was used for the Altair.

This figure shows Class A mishaps per 100,000 flight hours. Class A mishaps are defined as ones in which the aircraft is lost, death occurs, or \$1 million in damage is caused to the aircraft.⁷ This data shows that between 1998 and 2001 the number of mishaps per 100,000 flight hours for Predator was approximately 32. In comparison to the two other UAVs shown in the data, this is slightly more than half of the mishaps for the Hunter, and about a tenth of the mishaps of the Pioneer. When compared to piloted aircraft, 32 is quite a high number. For example, general aviation aircraft experience less than 1 and the F-16 approximately 3.5 mishaps per 100,000 hours. This is considered reasonable for a UAV, however, as there is an increased risk in using such technology.

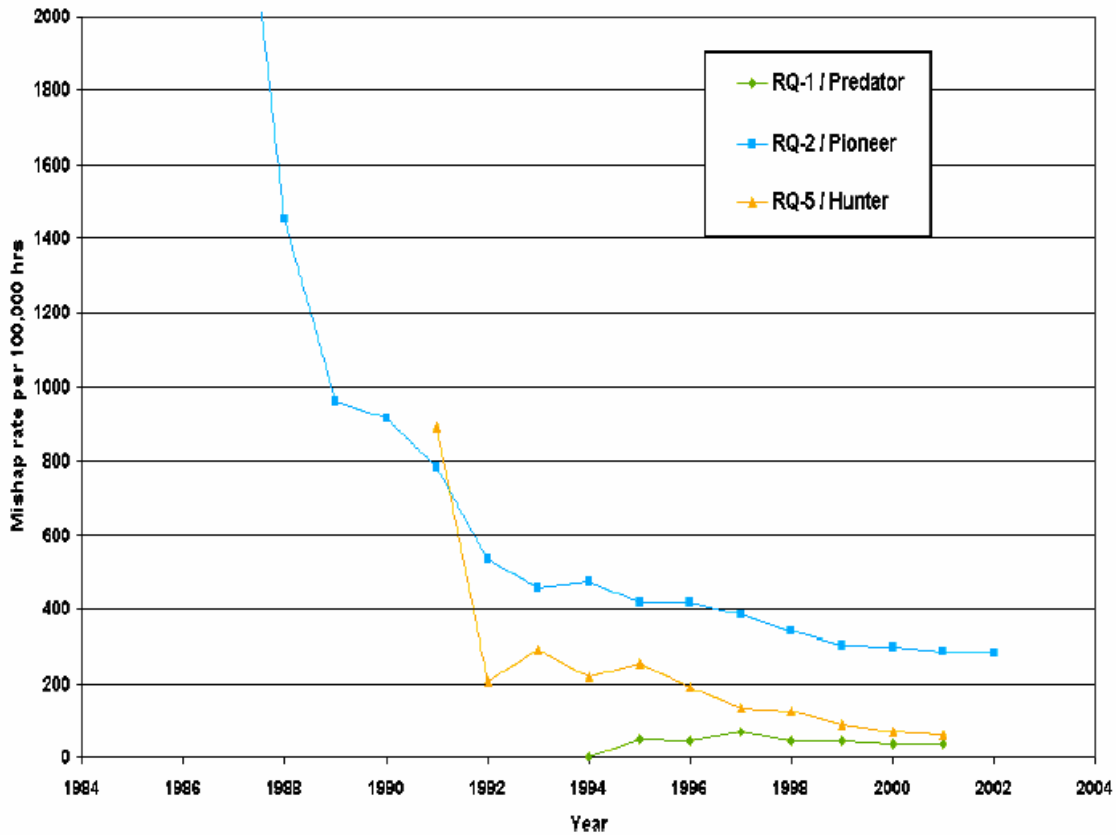


Figure 3 - Class A Mishaps per 100,000 flight hours⁸

Because of this high rate of Class A mishaps, it is necessary to determine what causes these failures and determine if the number can be reduced. Figure 4 shows the breakdown of the causes of these mishaps. The figure shows that 63% of the crashes are caused by either propulsion system failure or flight control failure.⁹ The incorporation of a parachute system, which can be deployed by the pilot or the copilot on the ground, would significantly reduce the number of mishaps caused by these failures.

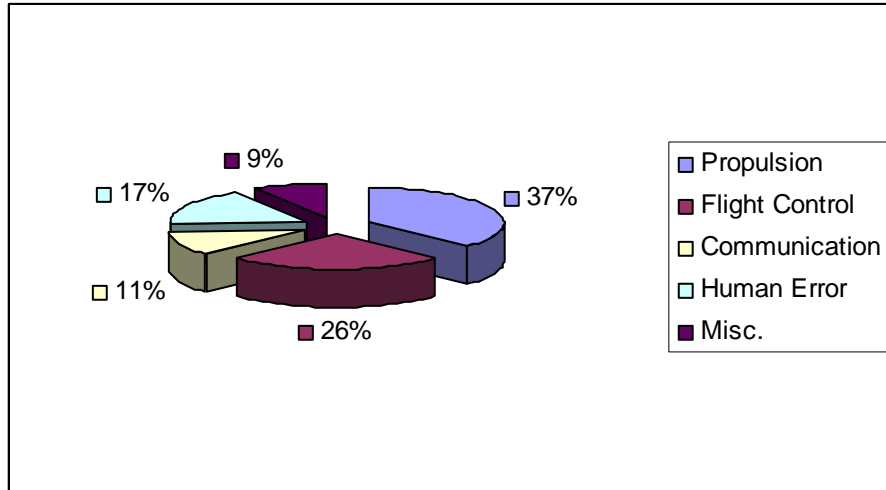


Figure 4 - Causes of UAV Class A mishaps¹⁰

III The Altair¹¹

III - A The Altair

The Altair is an unmanned aerial vehicle (UAV) capable of cruising at 144 knots airspeed at 50,000 ft for 32 hours. It has a single payload bay located in the front of the aircraft with 55 cubic feet total volume and a 660 lb weight capacity. The aircraft can also carry external payloads of up to 500 lbs.

Figure 5 shows a dimensioned side profile view of the Altair. The installation of a 100 lb payload may require, if not a tall strong individual, two short people with short ladders. The edge of the payload bay, with the top cover removed, is about 5 feet off the ground.

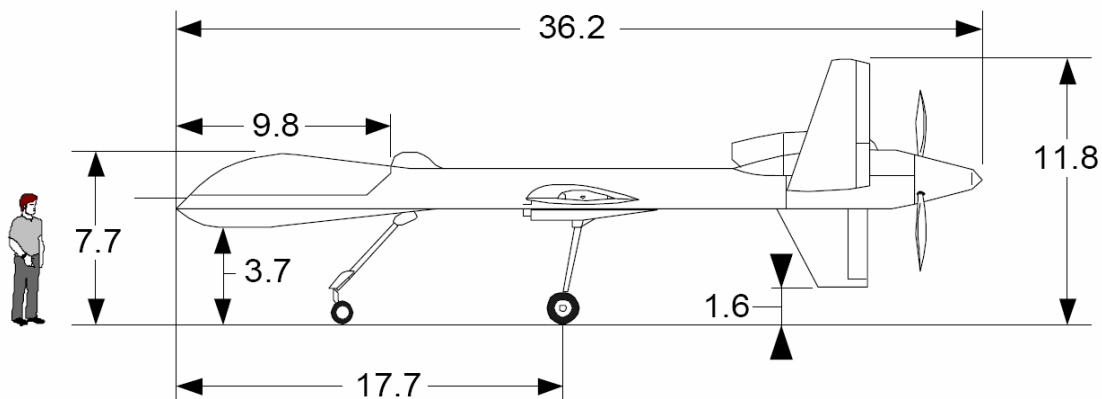


Figure 5 - The Altair

Figure 6 shows the external pod mounting locations. Up to 500lbs may be mounted in these locations, well beyond the weight of the MicroMAPS payload. Both power and data connections are available to external pod via close connections in the outside of the aircraft.

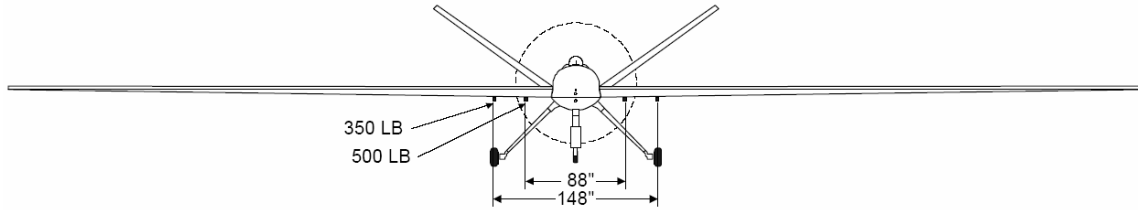


Figure 6 - External Pod mounting locations

III - B Altair Control Operations

The Altair is controlled by a ground control station (GCS) usually kept on or near the aircraft's point of departure, manned by a pilot and possibly a copilot. This station is a trailer which has pilot and copilot seats and payload linked workstations. The GCS communicates with the Altair through either C-band or Ku-band communication. C-band is a line of sight system in which data is transferred directly to and from the Altair, while Ku-band is a satellite communication system in which data is transferred through a satellite to and from the Altair (Figures 7 and 8).

Equipment in the payload bay of the Altair communicates with the GCS in real time. The download data rate for C-band datalink is 9.6 Kbps for payload data utilizing one uplink and two downlink data streams. The Ku-band download rate is twice that of the C-band and utilizes one uplink and one downlink data stream.

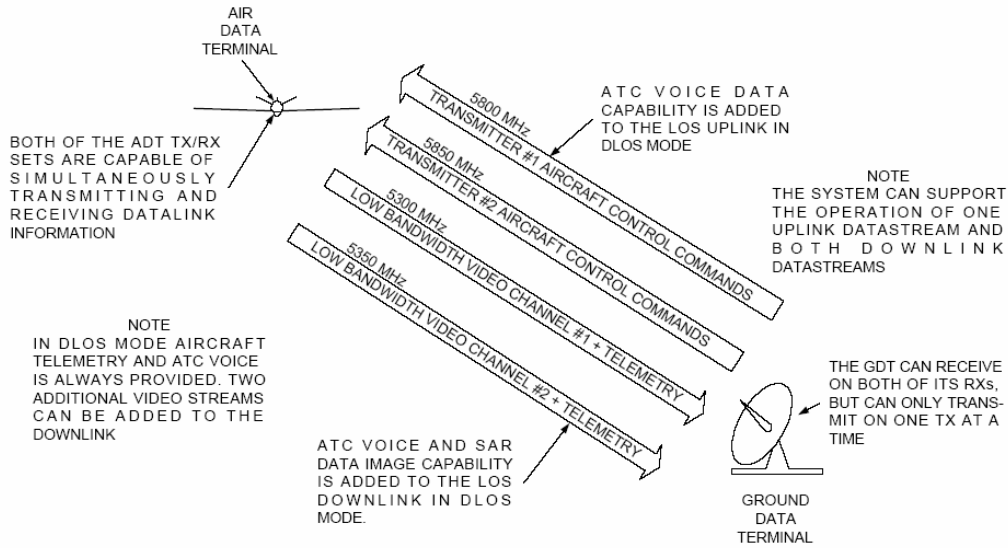


Figure 7 - C-Band Datalink Architecture¹²

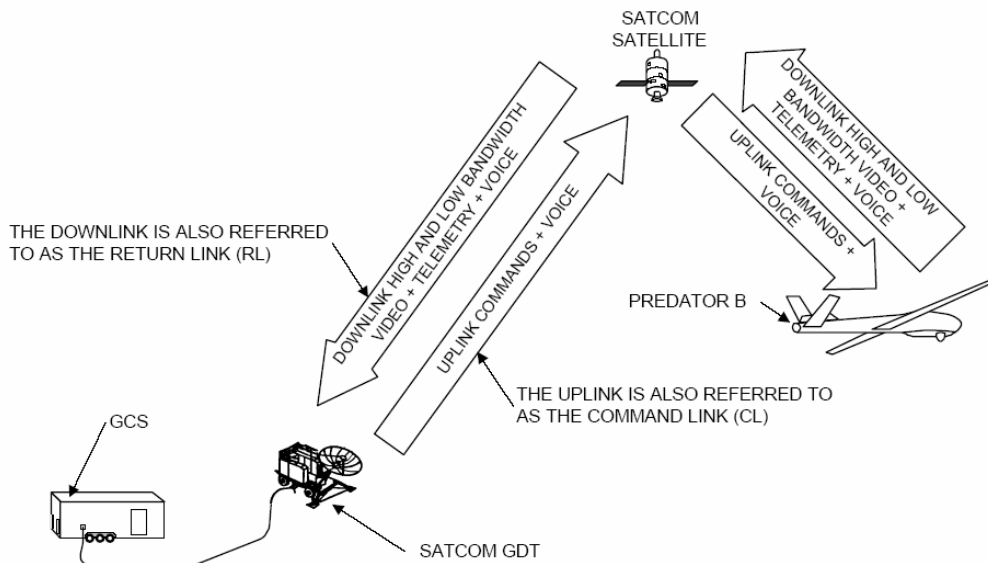


Figure 8 - Ku-Band Datalink Architecture¹³

The Altair was designed to perform real time, piloted missions, as well as autonomous missions. In both cases the aircraft is controlled by an FAA certified UAV pilot during take-off and landing. For real time flight, forward looking video is downlinked to the pilot in the ground control station. Autonomous flights are programmed by the pilot and initiated after takeoff. When the program is complete, the pilot then lands the aircraft in real time.

The MicroMAPS system can be controlled from the GCS by the pilots or NASA, using workstations installed in the GCS. Another option is using an adjacent trailer.

III - C Payload Installation

The Altair has a single payload bay in the front of the aircraft. This payload bay is about 5 feet off the ground. A ladder may be necessary to lift the payload into the payload bay. If necessary, an overhead winch may be used. The payload is about 100 lbs. Figure 9 shows the open payload bay with the desired location of the pressure vessel.

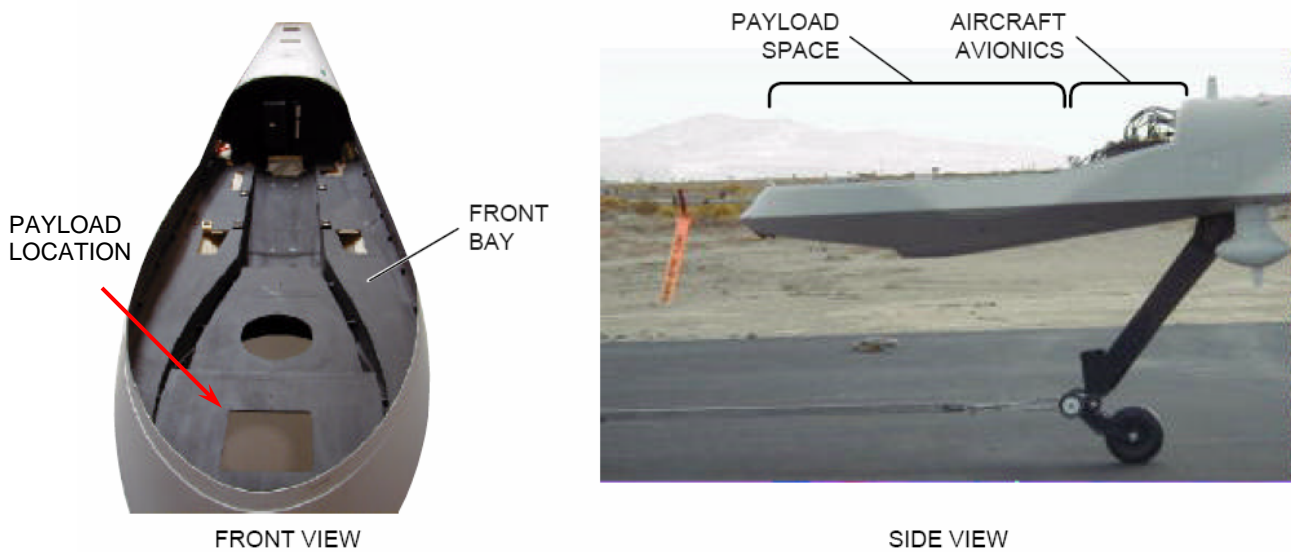


Figure 9 - Altair Payload Bay and Pressure Vessel Installation Location

IV Payload

IV - A Payload Overview

The entire MicroMAPS (pressure vessel and external shell) system will be made modular so that it can fly on multiple platforms. The electronics package will be designed for both an internal and external package that would be bolted down in the payload bay of the UAV or, if used as an external package, would be mounted in the external shell and then attached to the outside of the UAV or airplane. When mounting the entire system, it is important to select a location where MicroMAPS has a good line of site downward. The flying qualities of the aircraft should be minimally affected and the MicroMAPS must be easily accessible for maintenance and removal. There are several possibilities where the package could be mounted:

- The payload bay
- The fuselage at the CG of the UAV or airplane
- The exterior of the airframe (i.e. wing)

IV - B Internal Payload

To mount the electronics package in the payload bay of the UAV, we decided to encase it in a pressure vessel that can easily be bolted down. The MicroMAPS system will be mounted to an aluminum plate along with the power supply and the computer. A cover with a viewing window will be attached to the mounting plate to complete the pressure vessel. It will also have a pressure valve, electronic connections for data and power and a nozzle to fill the vessel with the desired gas. The cooling unit and the thermoelectric coolers will be attached to the exterior of the aluminum plate.

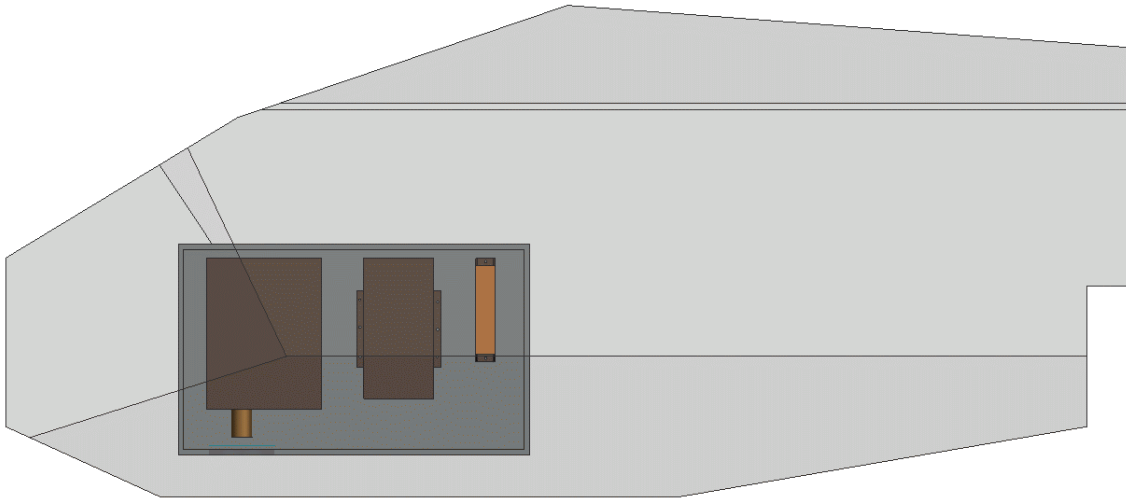


Figure 10 - Pressure Vessel Mounted in the Altair payload bay

IV - C External Payload

For external mounting, the pressure vessel will be encased in an aerodynamic shell that can be mounted to any vehicle either on the fuselage (at the CG) or on the wing mount. This external bay is available from Sargent Fletcher Inc.¹⁴ and will accommodate the pressure vessel (see Figure 11).

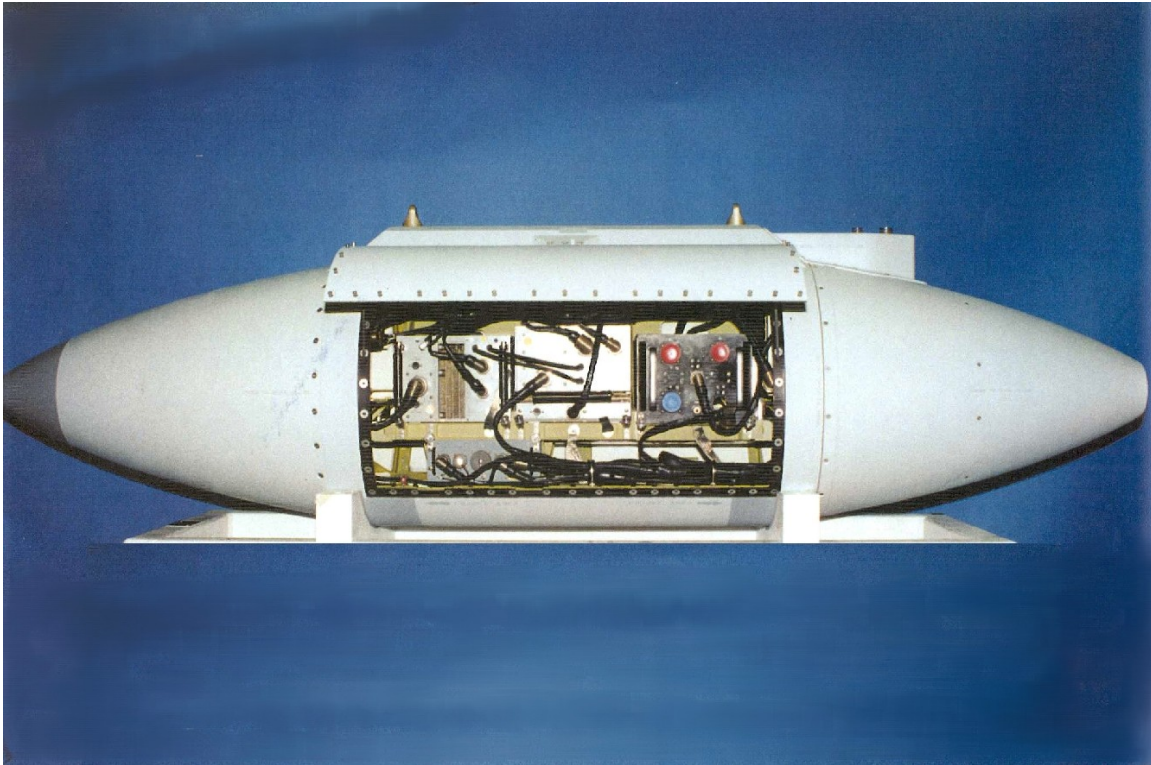


Figure 11 - External Pod Concept from Sargent Fletcher Inc.

IV - D Payload Weight

An estimated weight of the pressure vessel and its contents is shown in the table below. This total weight will consist of the MicroMAPS instrument, CPU, power supply, cooling system and the material of the pressure vessel container.

Cooling Assembly	~45 lbs.
MicroMAPS	14.33 lbs.
CPU and Power Supply	~5.0 lb.
Pressure Vessel	~35 lbs.
Total Weight	~100 lbs.

Table 2 - Approximate Payload Table of Weights

When calculating the entire weight of the pressure vessel a wall thickness of 0.15” was chosen. This is based on the results of the strength analysis described in section V -

C. With this wall thickness, the volume of the aluminum is approximately 360 in^3 . The following equation was used to calculate the weight of the empty pressure vessel.

$$W = \rho V$$
$$34.6\text{lb} = 0.096\text{lb}/\text{in}^3 \cdot 360\text{in}^3$$

The weight of the MicroMAPS instrument was cited in many sources that were used throughout the research. Weights of the components of the cooling assembly were also cited in the sources used to choose the components. The weights of the CPU and power supply were estimated.

IV - E Emergency Recovery Parachute

The team was asked to look into the possibility of an emergency parachute to recover the MicroMAPS payload. The most feasible option was to find an existing parachute system that had already been tested. The two possibilities were, first, to use a recovery system that would recover the entire UAV, or, second, to use a system that would recover only the payload.

There were no available systems that have already been designed and tested, capable of recovering the payload alone. In addition, a number of technical problems would arise if the team designed a system to eject the payload out of the UAV platform.

However, Butler Parachutes built a recovery system for the Predator UAV¹⁵ capable of recovering the vehicle at speeds of near zero and as high as Mach 2. Since the Altair and Predator are the same UAV platform, except for the wing span, this system should work on the Altair.

The Butler System uses a custom parachute bolted to the top of the airframe slightly aft of the center of gravity. When the system is initiated, a rocket fires and breaks

through the cover of the parachute compartment. The rocket tows the 70.5 foot diameter chute, causing deployment. The entire system weighs 76 lbs. including the attachment fittings on the UAV. When the parachute is deployed the UAV will have a descent rate of 18 ft./s.⁴

Butler's system has yet to be used in a real life scenario. Ground tests have been conducted along with a drop test from altitude using a simulated fuselage. Since this system will not affect the internal payload or an external payload it can be added to the UAV at any time during the project. MicroMAPS would require no modifications to accommodate the emergency recovery system.

V Pressure Vessel

V - A Design of the Pressure Vessel

The MicroMAPS instrument is very sensitive to moisture, and since the UAV is unpressurized, when the aircraft is descending, moisture will condense on the interior of the payload bay. To keep the instrumentation free of moisture, MicroMAPS, the computer, and the power supply all need to be enclosed in a sealed pressure vessel. The vessel must be capable of maintaining a pressure differential of 15 psi, which is the difference between atmospheric pressure at sea level and at 70,000 ft. The only part of the package not contained in the vessel is the cooling system.

The pressure vessel will be a reinforced rectangular prism, as shown in Figure 12. For the structural analysis, detailed in section V – C, a single beam welded across the inside top center of the box was used to reinforce the area with the greatest stress and reduce the required wall thickness. If desired, more reinforcement could be used to further reduce the weight. The rectangular prism shape was chosen because it is a simple shape to manufacture and it can enclose the instruments inside in the smallest possible volume. The increased minimum required wall thickness caused by using a rectangular vessel instead of a cylindrical one (and therefore increased weight) was not considered an issue because the overall payload weight will still be under the minimum required payload weight of the Altair. If need be, the pressure vessel can be enclosed in an aerodynamic shell and mounted on the exterior of the UAV. The MicroMAPS instrument, power supply, and computer will be mounted to a base plate covered by this rectangular prism as shown in Figure 12. The seal between the mounting plate and top will utilize a rubber gasket to maintain the internal pressure.

The pressure vessel must be sealed to maintain environmental integrity for the MicroMAPS instrument. The pressure vessel could be sealed by the use of a hinge connecting the mounting plate to the rest of the pressure vessel, with a gasket placed between them.

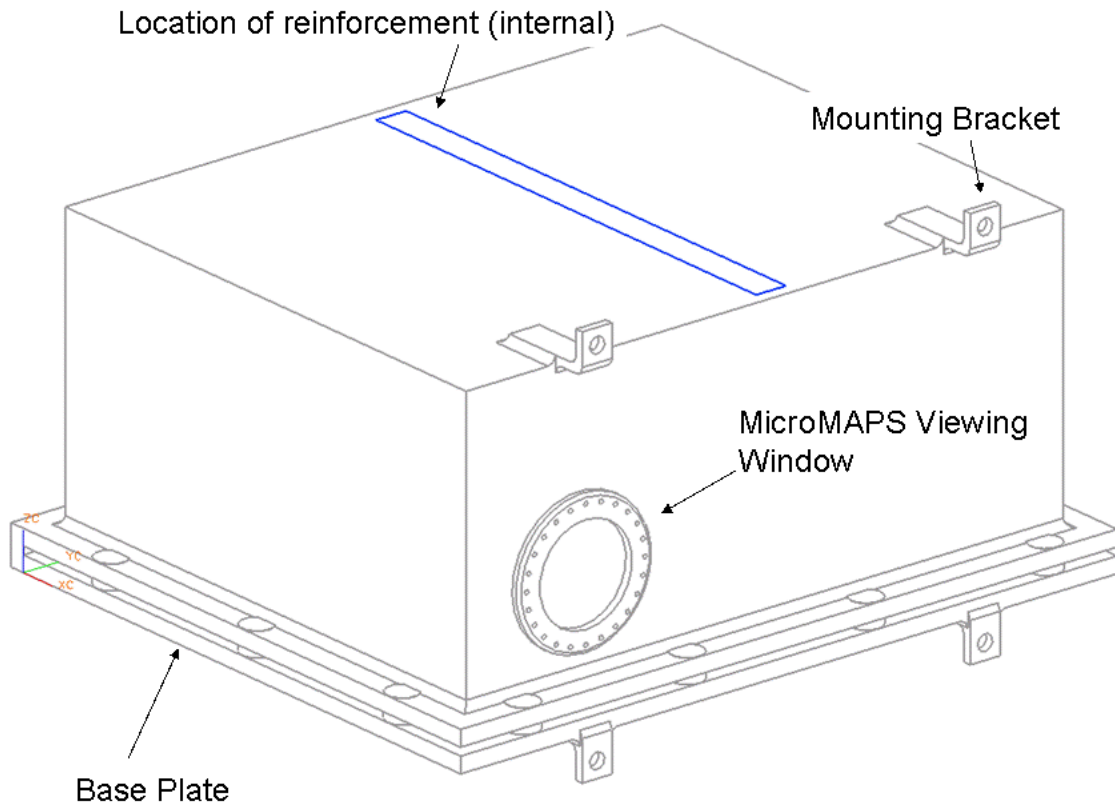


Figure 12 - Pressure Vessel

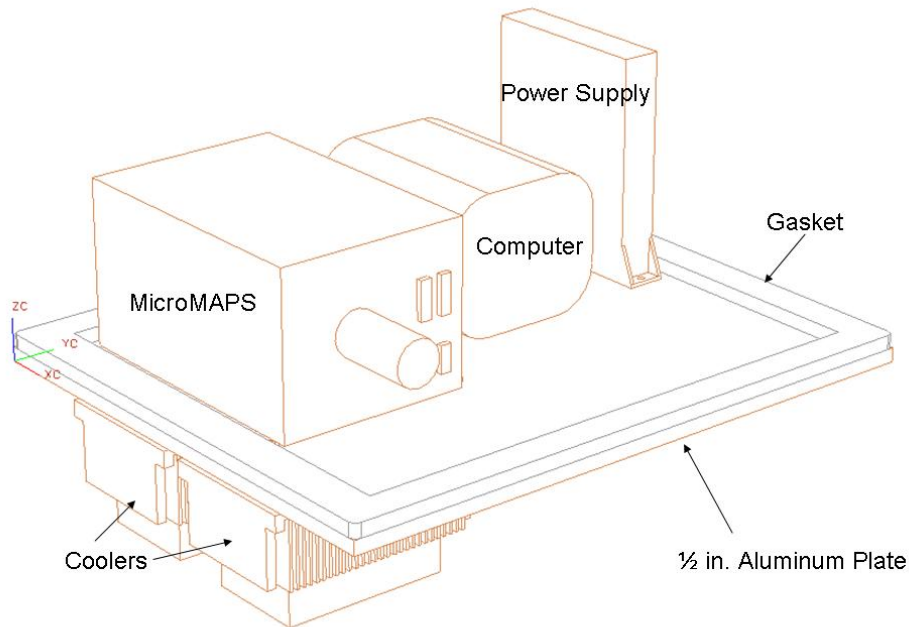


Figure 13 - MicroMAPS, Power Supply, and Computer on Pressure Vessel Base Plate

There will also be a viewing window at the bottom of the vessel. The specifications for this window have not been obtained from NASA yet, but this will not be a design issue as the viewing window was used for the Proteus flights in the summer of 2004.

V - B Pressure Vessel Material

The pressure vessel that will contain the MicroMAPS system, computer, and cold plate will be made of aluminum alloy 2014. A few materials were considered for the pressure vessel before deciding on aluminum. They included steel, transparent and opaque plastics and composite material. The decision to use aluminum was made because it is a light but strong material that can withstand cold temperatures, is commonly available and is easy to work with.

After deciding to use aluminum as the material for the pressure vessel, the specific alloy selected for the project was aluminum alloy 2014. An alternative is a less expensive and weaker, but more commonly available, aluminum alloy 6061. The physical properties of these alloys are listed in the Table 3.

Table 3 - Physical Properties of Aluminum Alloy 2014 and 6061

Material Properties	Density (lb/ft ³)	Young's Modulus (in ⁶)	Poisson's Ratio	Yield Strength (lb/in ²)	Ultimate Strength (lb/in ²)
Aluminum 6061	0.452	10,000,000	0.33	35000	40001
Aluminum 2014	0.438	10,600,000	0.33	57151	64001

Both alloys do not require heat treatment but may be strengthened using strain hardening or annealing. Aluminum is highly resistant to corrosion which makes for a good material for long term outdoor use. It is also good for welding, an important quality for the manufacturing process.

V - C Pressure Vessel Shape and Thickness

Two shapes were considered in designing the pressure vessel, a cylindrical tank with spherical caps and a rectangular box. The decision to use a rectangular shape was based primarily on ease of manufacturing and cost. This did increase the weight, however, as all the components inside are rectangular, it allowed for smaller overall dimensions.

V - C - 1 Wall Thickness Calculations

To determine the minimum required thickness of the pressure vessel, rough calculations were performed first by hand, simplifying the problem to a 19 inch beam

with clamped ends. Equations (1) and (2) below were used and predicted the minimum thickness required. An engineering safety factor of 2 was chosen because, as the primary load on the payload will be caused by pressure, it is impossible to exceed the stress due to one atmosphere (about 15 psi). Additional stress could be seen during landing. This force, however, will come from primarily the equipment inside the pressure vessel which will act upon the base plate and subsequently the base plate mounts (see Figure 13) rather than the pressure vessel walls.

One wall of the pressure vessel can be modeled as a uniformly loaded beam clamped at both ends. In this case, the maximum bending will occur at the center of the beam. In the real pressure vessel, the ends will be welded and will be somewhat flexible which will decrease some of the stress through the wall. To solve for the minimum thickness that the pressure vessel can withstand without yielding, the following equations were used¹⁶:

$$\sigma_{\max} = \frac{M_{\max}}{S} \tag{1}$$

$$S = \frac{I}{c} = \frac{\frac{1}{12}bt^3}{t/2} \tag{2}$$

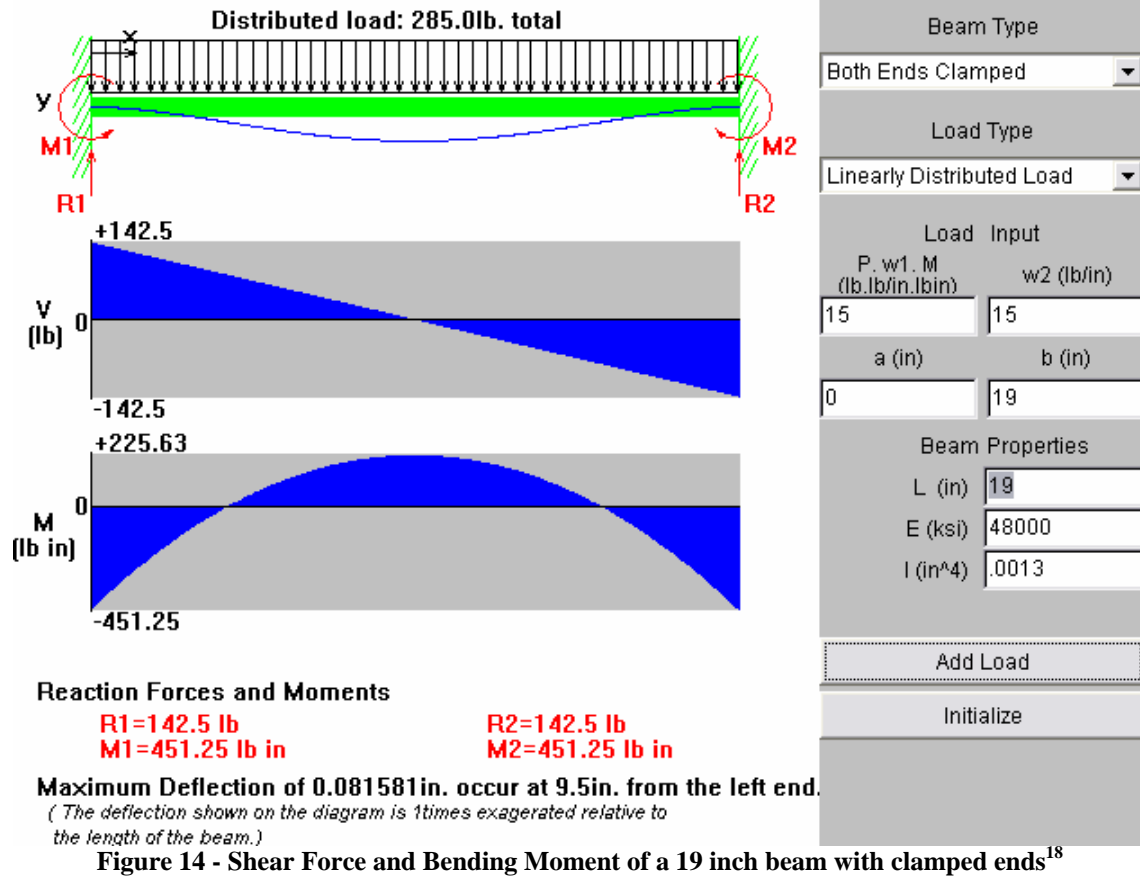
The following table is a summary of the hand calculations.

Table 4 - Pressure Vessel Minimum Required Wall Thickness Estimate.

Length of longest side	L = 19 in
Uniform load	P = 15 lb/in
Maximum bending moment	M _{max} = 225.63 lb-in
Maximum yield stress	σ _{max} = 40,000 lb/in ²
Minimum wall thickness	t = 0.260 in

Using a factor of safety of 2, the minimum thickness that the pressure vessel walls can withstand without yielding is 0.26 in. This process was not done for all six sides of the vessel because the longest side will have the largest moment due to bending.

Now that the minimum thickness is determined the shear stress and bending moment diagrams can be plotted. To do this the java application called “Beam View: Beam under Transverse Loads¹⁷” was used. Figure 14 shows the plots of the distributed load, shear force and bending moment as each varies with length. On the right, the input information shows the beam type, load type and load that applied to the problem. In addition the length of the beam, moment of inertia and Young’s modulus for the pressure vessel material were entered. Below the graph of the bending moment the shear and bending moment are given for the beam. Using this analysis, the maximum deflection of the center of the beam is 0.082 inches. With such a small deflection fatigue stress is not a concern as it would take thousands of flights to reach failure.



A more exact solution for the minimum required wall thickness was obtained through the use of a finite element software package, ANSYS. This software uses models exported from a CAD program such as Unigraphics and, after the application of boundary conditions and material properties, outputs the stress, deflection, and safety factor of the model. The same model that was used for the temperature variation analysis in CFDesign was used for the finite element analysis with the addition of a support beam across the top center of the vessel. This beam was intended to reduce the maximum deflection (by more than 60%) and therefore the maximum stress and to reduce the required thickness. A pressure difference of minus 15 psi was applied to the outside of the pressure vessel. Two commonly available alloys of Aluminum were used in the analysis, Al 2014 and the weaker, Al 6061. Figure 15 shows the stress distribution on the base plate and Figure 16

shows the stress distribution and deflection over the upper surfaces. The deflection here is significantly exaggerated for clarity. A summary of the results is shown in Table 5. Using the 2014 alloy, the minimum thickness required for a safety factor of 2 is about 0.15 inches. For 6061 the minimum thickness of 0.25 inches, is just slightly under the hand calculation estimates. The weight of the pressure vessel is 35 pounds with a wall thickness of 0.15 inches and 50 pounds for 0.25 inches. Regardless of the wall thickness, the base plate is assumed to remain at 0.5 inches. This over-designed base plate was used in the Proteus design and proved useful when the payload was dropped during delivery. In case of such an event, a half inch base plate is still recommended, however not required.

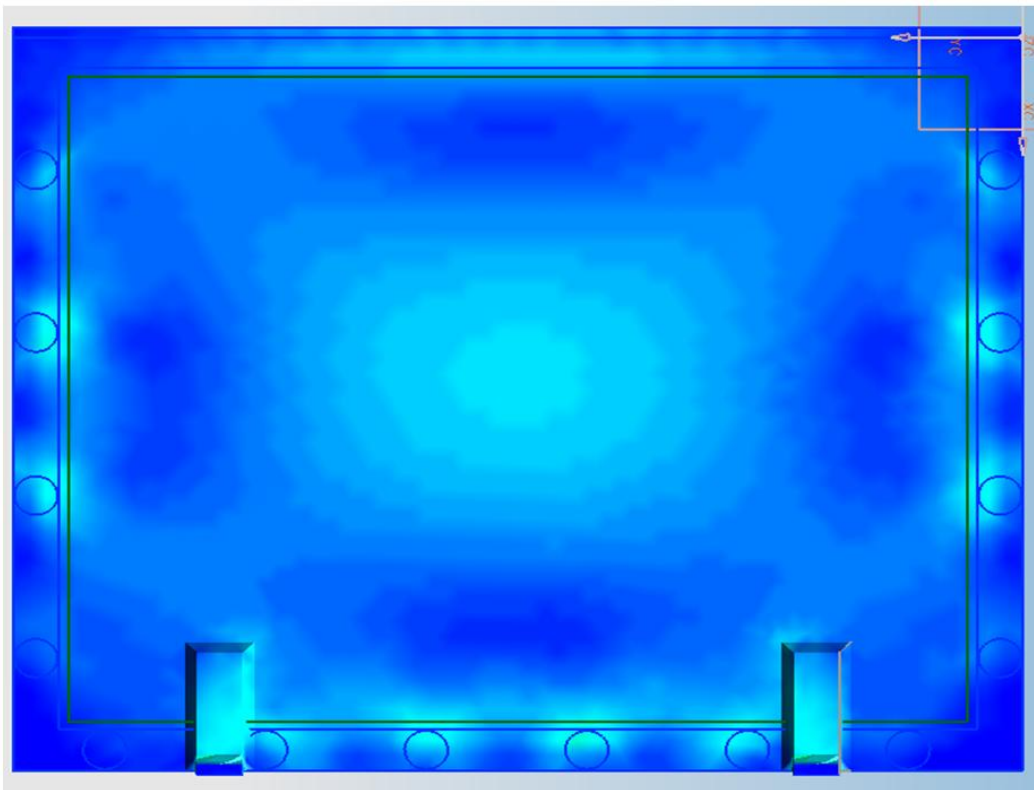


Figure 15 - Base Plate stress distribution at 15 psi

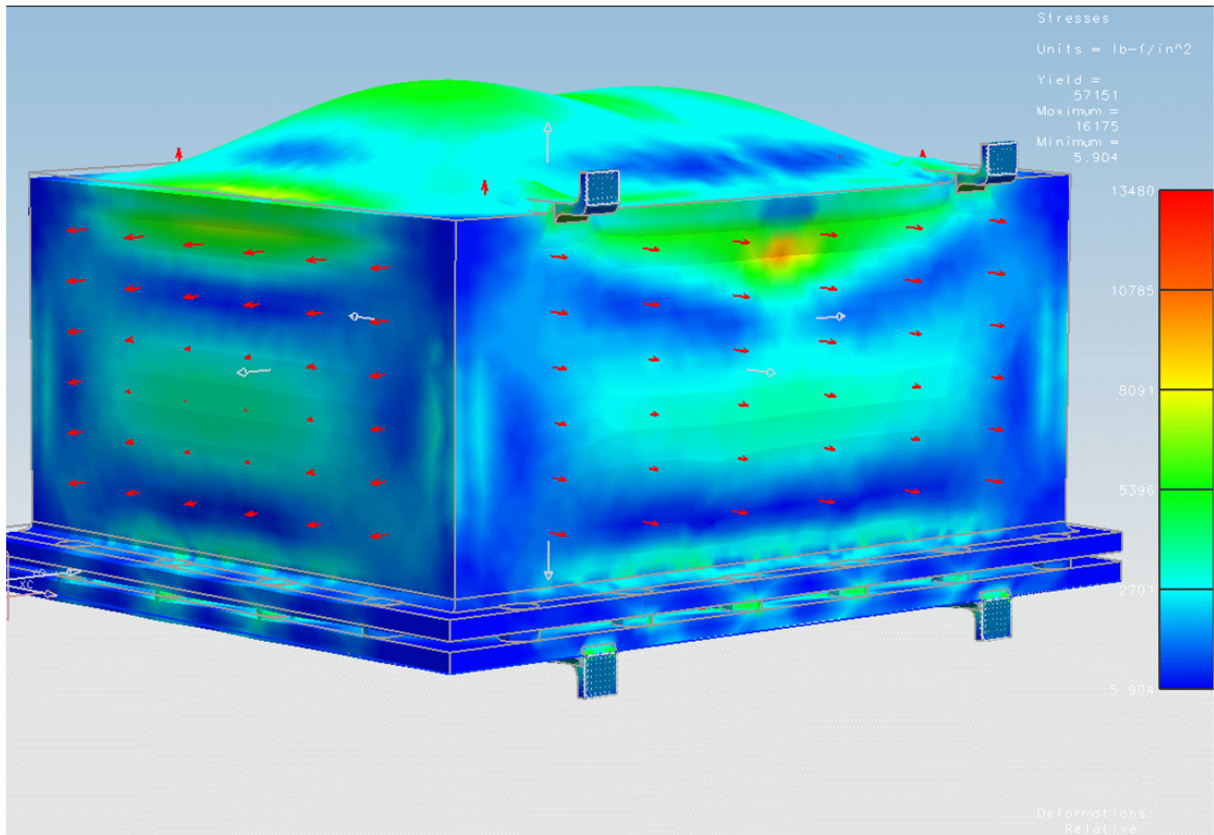


Figure 16 - Pressure Vessel Stress Distribution at 15 psi

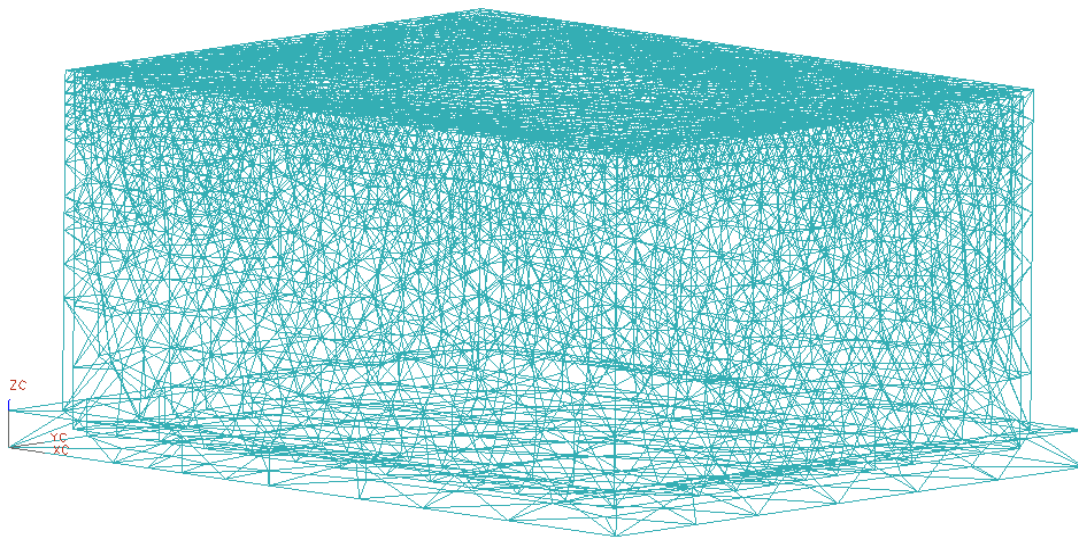


Figure 17 – Stress Analysis Mesh

Table 5 - FEA Analysis Summary

Wall Thickness in.	Material (aluminum)	Weight (Lb)	Volume (in ³)	Maximum Stress (psi)	Maximum Displacement (in.)	Factor of Safety (minimum)
0.18 inch	6061	40.07	409	27680	0.3825	1.264
	2014	41.00			0.3610	2.116
0.20 inch	6061	43.79	447	24408	0.2599	1.434
	2014	45.13			0.2452	2.341
0.25 inch	6061	48.59	496	16068	0.1336	2.178
	2014	50.07			0.1261	3.557
0.375 inch	6061	60.49	618	15446	0.0382	2.266
	2014	62.34			0.036	3.700
0.5 inch	6061	73.18	747	15515	0.0271	2.256
	2014	75.42			0.0255	3.684
Reinforced Pressure Vessel:						
0.18 inch	6061	43.31	442	23018	0.0899	1.521
	2014	44.63			0.0848	2.483
0.20 inch	6061	45.25	462	21526	0.0714	1.626
	2014	46.63			0.0673	2.655
0.25 inch	6061	50.08	511	16175	0.0444	2.164
	2014	51.61			0.0419	3.533
0.375 inch	6061	62.09	634	15447	0.0273	2.286
	2014	63.99			0.0258	3.700
0.5 inch	6061	73.99	775	14722	0.0271	2.377
	2014	76.25			0.0255	3.882

The wall thickness of the pressure vessel is extremely important. This design places more importance on the safety of the equipment than the overall weight, since this is the only instrument in existence.

There are two possible ways to construct the rectangular pressure vessel. Either the corners of the rectangular box are going to have a slight bend in them, or the corners will be straight and welded together. If the aluminum is bent, then the inside radius could be too small and cracking could occur. The cracking usually is more distinct when the bend runs parallel to the natural grain of the material. To help with this problem, it is advantageous to make the inside radius of the bend at least equal to or greater than the material thickness. If the corners are welded then the welds will need to be tested to make

sure they can withstand pressure being contained in the vessel. In the ANSYS model, the corners were modeled with 0.25 radius welds on the inside corners.

V - D Pressure Connectors

It is important to maintain a stable environment inside of the pressure vessel. Ideally there would be no entry and exit holes in the pressure vessel. However, since there are electronic devices requiring power inside the vessel, holes are necessary. To maintain the pressurized environment a pressure connector will be mounted. A pressure connector is a long cylindrical connector with a connector on both ends. One end is in the pressurized environment and the other end is in the open air.

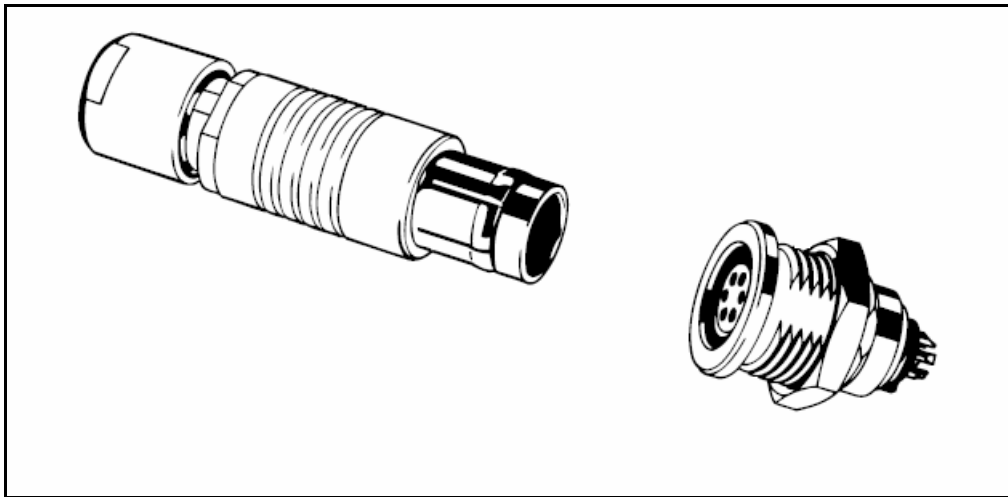


Figure 18 - Fischer Co. Pressure Connector (example)¹⁹

For MicroMAPS two of these connectors are necessary. One will send power to the computer, and the other will carry MicroMAPS data. The Fischer Company has a large variety of pressure connectors to choose from. The company tests the connectors with a hydraulic pressure of 8000lb/in² and leaves them pressurized overnight.

V - E Pressure Valves

There will need to be three valves: one pressure release valve, one inlet and one outlet valve for purifying the chamber. The purpose of the valves is to release air from the vessel and add a dry gas of known qualities into the vessel. The valve will be designed by a third party company, such as SMC Corporation of America, which makes a variety of acceptable valves²⁰. A ball type valve will be used, directly welded to holes in the vessel. An example is shown in Figure 19 courtesy of the Valve Shop.²¹



Figure 19 – Ball-type valve from *The Valve Shop*²¹

V - F Gasket Design

Several rubber companies were contacted about manufacturing the gasket, including United Seal and Rubber²², and Aero Rubber Company, Inc.²³. Unfortunately, the cost of manufacturing very small quantities of a custom gasket is prohibitively high. All the companies contacted either refused to manufacture the gasket or suggested another company.

Our suggestion, therefore, is to fabricate a piece of rubber to serve as the gasket. It would be the same outside dimensions as the mounting plate, 1 inch wide and 5 mm thick.

VI Thermal Management

VI - A Temperature Requirements

Electronic components are sensitive to temperature. Their performance is restricted to a specified temperature range, and the component may be destroyed if the temperature exceeds the range. The operating temperature is specified by the manufacturers and usually ranges from zero to 70°C (industry), -20°C to 85°C (civil), and -55°C to 125°C (military).

Temperature can be a limiting value beyond which operation is not guaranteed. Severe temperature variation may cause a reduction in the performance and eventually lead to failure due critical temperatures at which state changes occur. The contraction and expansion of the constraints in materials are caused by the variant temperature and can lead to failures. The objective of cooling the electronic components is to maintain the temperature of each element at its nominal operating temperature.

A major obstacle to the MicroMAPS implantation on the Proteus is the absence of thermal management of the electronic devices. The system is not equipped with a cooling or heating system and then is subjected to the fluctuation of the external flight temperature. The MicroMAPS system has been confronted with high temperature on the ground and extremely low temperature during the data acquisition. These considerable changes in temperature may have some major consequences on the lifetime of the system. Moreover, in order to begin the data acquisition and obtain accurate results, the temperature must stay constant in the instrument enclosure, resulting in a delay of 4 hours after the take off.

As shown by the following graph, the temperature in the payload bay of the Altair ranged from 104 °F to 39 °F. If installed in the payload bay, the MicroMAPS will be exposed to a smaller range of temperature than using the Proteus, and the system temperature will tend to slowly converge to approximately 50°F.

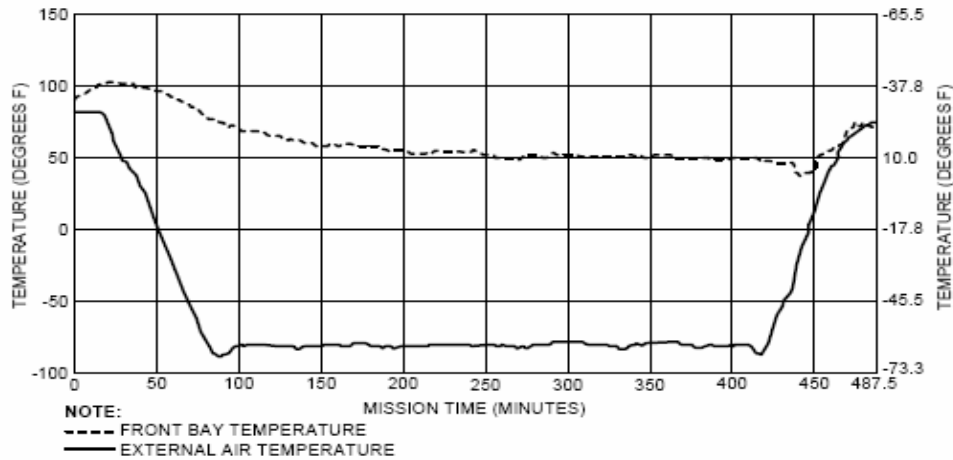


Figure 20 - Temperature Variation in the Altair Payload Bay²⁴

Therefore, the goal is to design a system able to quickly change the system temperature to 50°F and keep it constant during the flight. Having a thermal management control system on the Altair will lead to an increase of the system lifetime, a considerable reduction in the time required before initiation of data acquisition, and a reduction in data cost.

This section provides a description of the thermal analysis of the MicroMAPS/pressure vessel assembly. A better understanding of the heat transfer and the thermal distribution is necessary for the design of a heating/cooling system able to quickly change the system temperature to 50°F and keep it constant during the flight.

VI - A - 1 Unsteady state condition

A numerical method to calculate the temperature distribution and heat transfer for equilibrium conditions is easily solvable but inaccurate results will be obtained. If the enclosure is suddenly subjected to a change in environment, some time will elapse before an equilibrium condition will prevail in the body. The system becomes an unsteady heat transfer problem. The analysis must take into account the change in the internal energy with time, and the boundary conditions must be adjusted to match the actual physical situation of the system.

Natural convection in enclosures is driven by the buoyancy force. Not many published materials exist on the subject of natural convection in an enclosure with a localized heat source due to the complexity of the problem. However, numerical simulation of transient laminar natural convection in a rectangular enclosure with a localized constant heat flux source is obtained by the SIMPLE (Semi-Implicit-Pressure-Linked-Equation)²⁵. Studying numerically the effects of heater size, location, aspect ratio for a rectangular enclosure with constant temperature heat sources is very challenging and might be irrelevant to our design process. In our case, we have a variable heat load with non constant heat sources. In order to simplify our analysis we decided to use CFD Design which is a fully interactive software tool, used for thermal management by design engineers in the electronics industry by predicting air flow and heat transfer.

VI - B Thermal Model Description

The thermal model consists of the MicroMAPS, the computer, and the power supply enclosed in a sealed pressure vessel. The pressure vessel should be able to maintain a pressure difference of 15 psi.

Aluminum alloys are well known to have a strong resistance to corrosion as a result of an oxide skin that forms a corrosive protection from most chemicals and weathering conditions. In addition, they are also known to have good electrical and thermal conductivities. These electrical and thermal properties, listed in Table 6, make aluminum alloys very useful as thermal conductor and for cooling applications.

Alloy	Coefficient of Thermal Expansion 20° - 100°C μm/m-°C	Thermal Conductivity at 25°C W/ m-K	Electrical Conductivity % of Cu 20°C		Electrical Resistance 20°C	
			Equal volume	Equal weight	Ohm-cmil/ft	Ohm-cm x 10-6
5083	23.76	117	29	98	36	5.98

Table 6 - Properties of Aluminum Alloys²⁶

As shown in the following figure all the electronics will be mounted on an aluminum plate. Inside the pressure vessel, are located the MicroMAPS, the computer, and the power supply. On the external side of the cold plate the cooling system is mounted. In this way the thermo-coolers will extract the heat out of the pressure vessel directly from the instrument, through the aluminum plate and the walls (for more detail, see section VI – D).

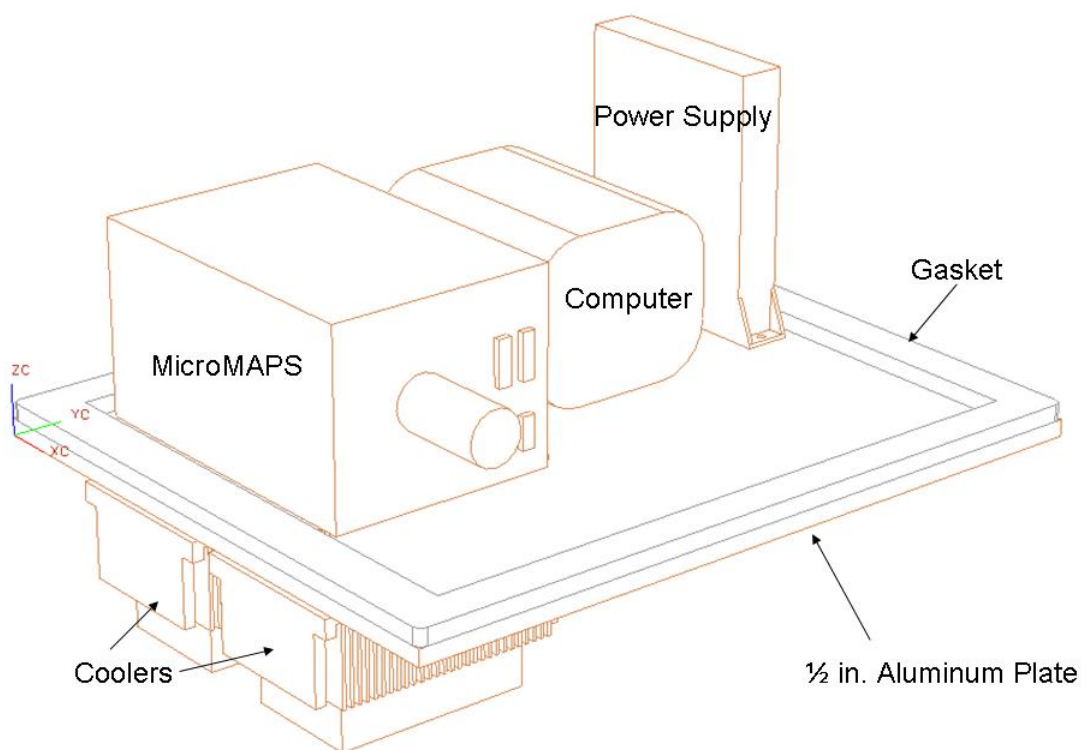


Figure 21 - Model used for Thermal Analysis

Figure 11 shows a simplified representation of the MicroMAPS instrument and pressure vessel assembly. For the thermal analysis, the pressure vessel was considered to be a closed system since there is no mass transfer into or out of the vessel. The gas inside was considered an ideal gas and constant specific heats were used. The volume of the vessel is also constant

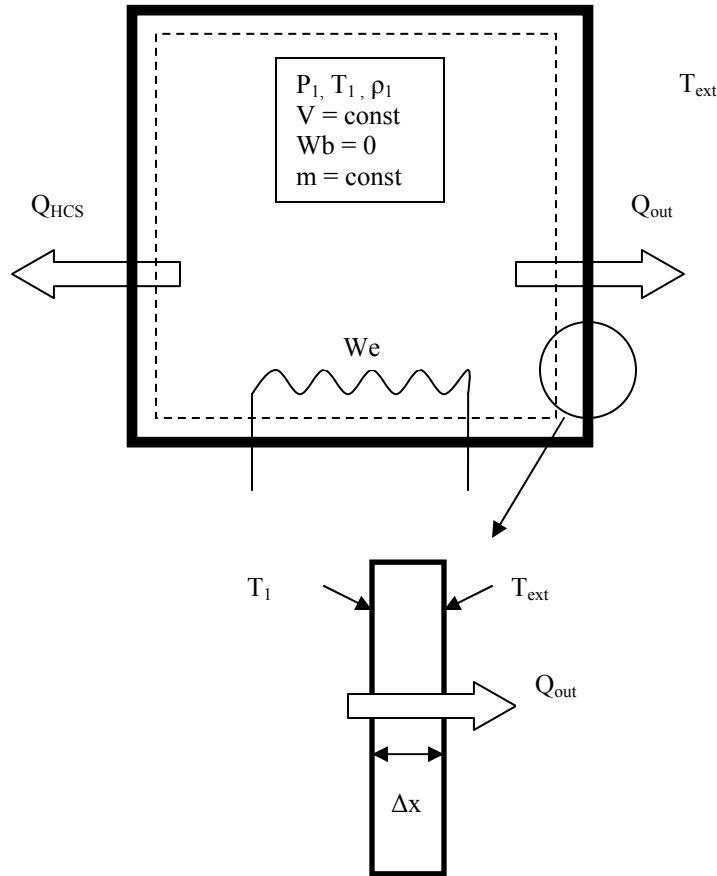


Figure 11. Thermal model and conduction process

VI - B - 1 Conduction

Conduction is the transfer of energy from the more energetic particles of a substance to the adjacent less energetic ones. The rate of heat conduction dQ/dt through a layer of constant thickness Δx is proportional to the temperature difference ΔT across the layer and the area A normal to the direction of heat transfer, and is inversely proportional to the thickness of the layer²⁷.

$$\frac{q}{A} \int_{x_1}^{x_2} dx = -k \int_{T_1}^{T_2} dT \rightarrow \frac{q}{A} = \frac{k}{\Delta x} (T_1 - T_2)$$

This relation is called Fourier's Law, it is used for steady-state heat transfer when the thermal conductivity of the wall k is assumed constant.

VI - B - 2 Natural Convection

In Natural convection, also called free convection, density differences propel fluid motion caused by temperature differences within the fluid. Gravity causes the heated and less dense fluid to rise while the cooler and more dense fluid to fall. In an enclosure such as the one design for the MicroMAPS, the Nitrogen fluid will form circular flow paths as the heated gas rises, begins to cool and fall, and is then heated to rise again, as described in next figure.

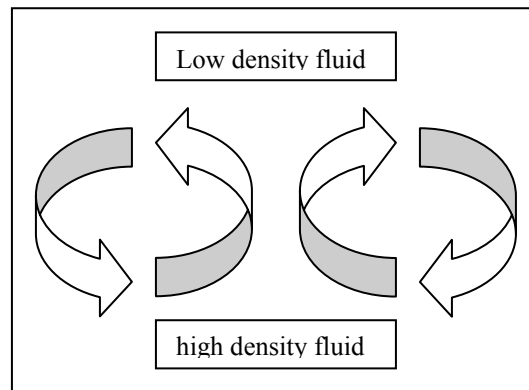


Figure 22 - Natural Convection

Since the fluid motion is small and the velocities are low, resulting in much less mixing, the heat transfer coefficient in natural convection is much smaller than in forced convection. For these reasons, we can expect in our case, that conduction effects will dominate the heat transfer process.

VI - C Temperature Analysis

VI - C - 1 CFDDesign

CFDesign is a user friendly computational fluid design program. It was used to visualize, understand and optimize the heat transfer throughout the pressure vessel.

Simplified models of the pressure vessel and payload bay were exported from the CAD software Unigraphics and imported into CFDDesign. Multiple simulations were assembled and run.

Once the model is opened in CFDDesign, boundary conditions, mesh sizes and material properties are set. The software automatically produces an optimized mesh and initializes the simulation. CFDDesign's dynamic and interactive display can be used to monitor the progress of the simulation as it works toward a converged solution. Time varying initial conditions were used to model the heat production of the computer and MicroMAPS, the heat removed with the cooler and the outside temperature variation as the aircraft climbs to altitude. The temperature of the MicroMAPS instrument was used to determine adequate temperature stabilization. As shown in Figure 23, three monitor points were chosen on three different surfaces of the instrument in order to verify the temperature.

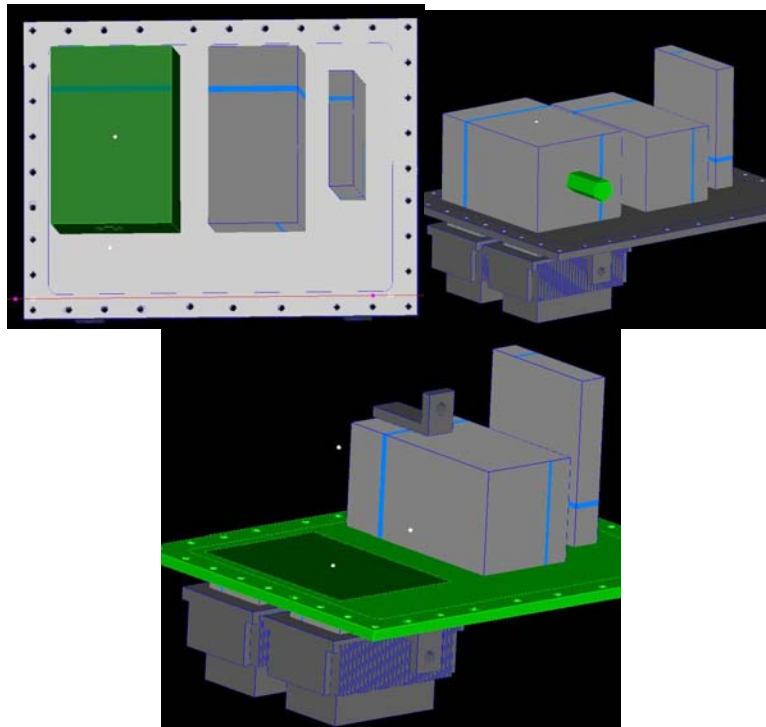


Figure 23 - CAD Model Used for Thermal Analysis, some parts omitted

VI - C - 2 Initial and Boundary Conditions

The temperature in the payload bay of the Altair ranges from 104 °F to 39 °F. The payload bay temperature converges slowly from relatively high temperature 104 °F (40°C) to approximately 50°F in 3 to 4 hours. These temperature conditions are the maximum that can be expected. In other words, we will design the cooling system such that it can be efficient in these particular conditions, which we expect to be the conditions with the higher payload bay temperature. We also assumed that the initial temperature of each component will be, in the worst case scenario, 104 °F (40°C).

VI - C - 3 Without any cooling system

During this heat analysis, our first objective was to define and simulate the temperature variation of the system if no cooling system is used. The following graph illustrates the temperature versus time of the cylindrical part of the MicroMAPS in front of the viewing windows.

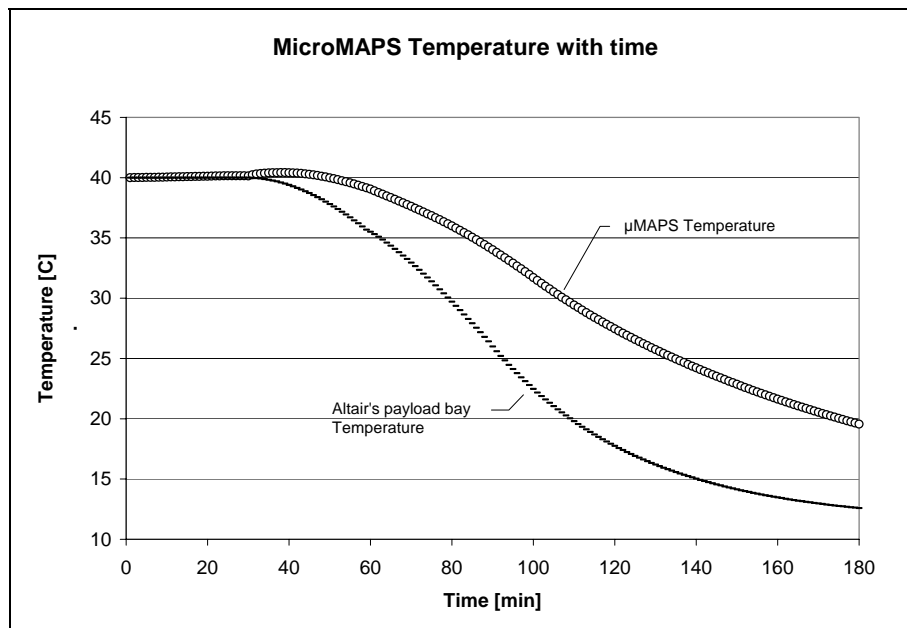


Figure 24 - Temperature Variation without cooling

As shown in Figure, the temperature inside the pressure vessel remains constant at 40°C for almost 1 hour after take off. This can be explained by the fact that for the first minutes in flight the payload bay is also about 40°C. Then the heat added to the system by the MicroMAPS, the computer and power supply helps to keep the temperature high in the pressure vessel even while the internal payload bay temperature of the Altair is decreasing. Next, the temperature of the payload bay is inferior to the temperature inside the pressure vessel. This difference of temperature through the walls of the pressure vessel leads the dissipation of the heat by conduction. This process is slow; the rate of change in temperature is illustrated in Figure 14.

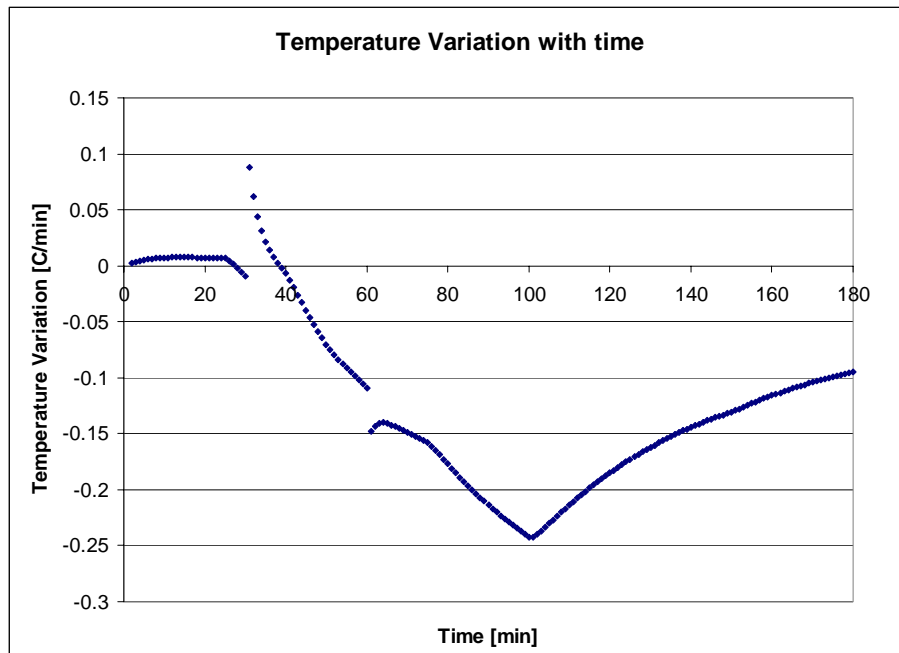


Figure 25 - Rate of Temperature Change inside Pressure Vessel without cooling

The rate of change in temperature is at its maximum, $-0.25\text{ }^{\circ}\text{C}$ per minute at 100 min after takeoff. The temperature change value obtained after 3 hours is at approximately $-0.1\text{ }^{\circ}\text{C}$ per minute. The severe change in the slop of this curve can be

explained by the change in some of the boundary conditions like the heat removal of the coolers.

Figures 24 and 25 show that it will take more than 3 hours to obtain a relatively stable temperature inside the pressure vessel (approximately 15 °C), and to begin the data acquisition.

VI - C - 4 Thermoelectric cooling assembly location

The models shown in Figure 15 illustrate the temperature variation with time of the aluminum plate on which are mounted the several components in the pressure vessel.

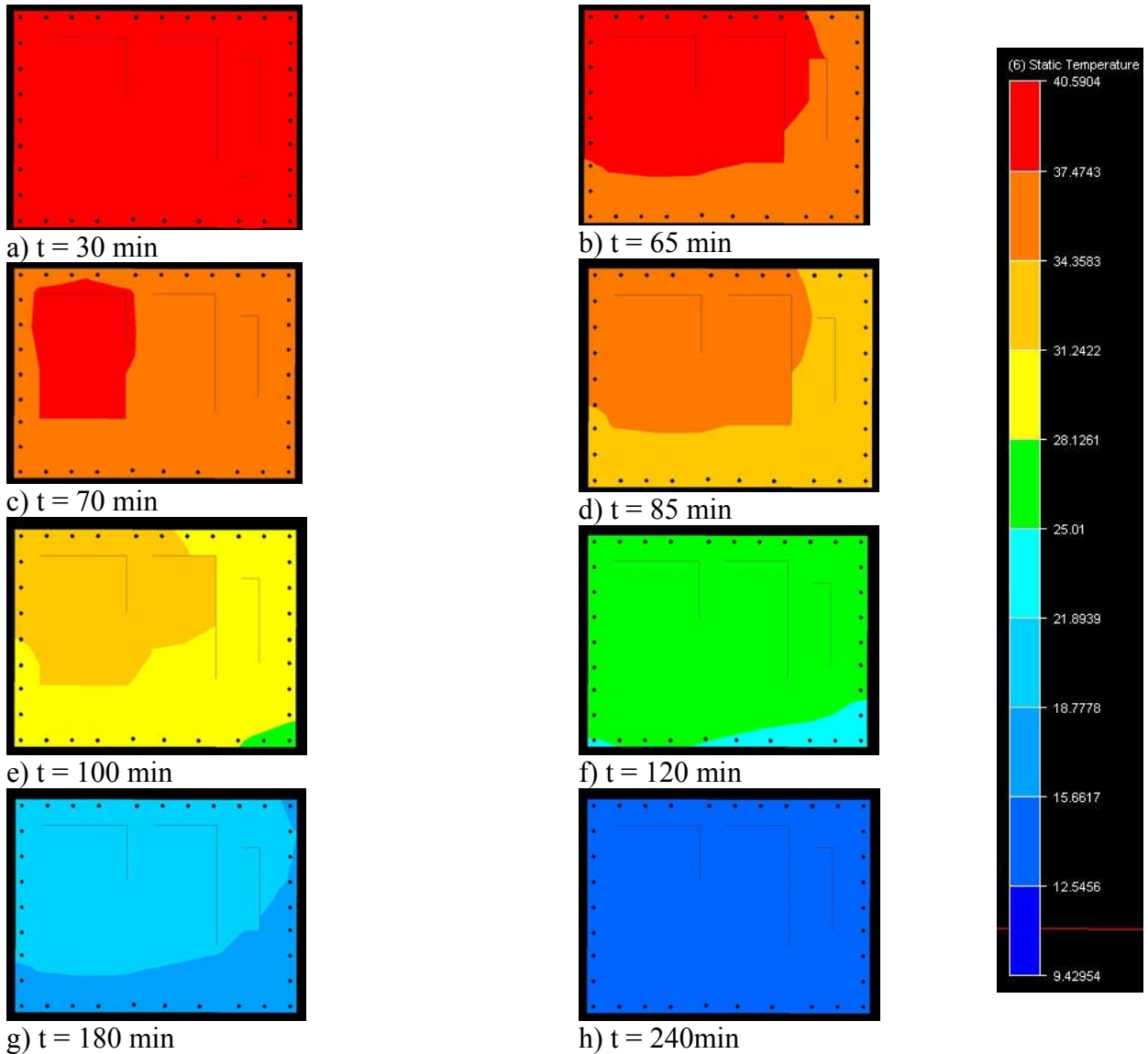


Figure 26 - Base Plate Temperature Variation (°C) without cooling.

These figures demonstrate that MicroMAPS is the major source of heat in this system. It can be seen that, at any specified time, the area above MicroMAPS describes the region of the aluminum plate where the temperature is the largest. Thus, in order to

maximize the cooling process efficiency, the thermo-coolers will be mounted under MicroMAPS on the external face of the aluminum plate. This aluminum plate will serve as a cold plate and will diffuse the heat removal to the internal part of the pressure vessel.

VI - D Thermo-electric Cooling Assembly

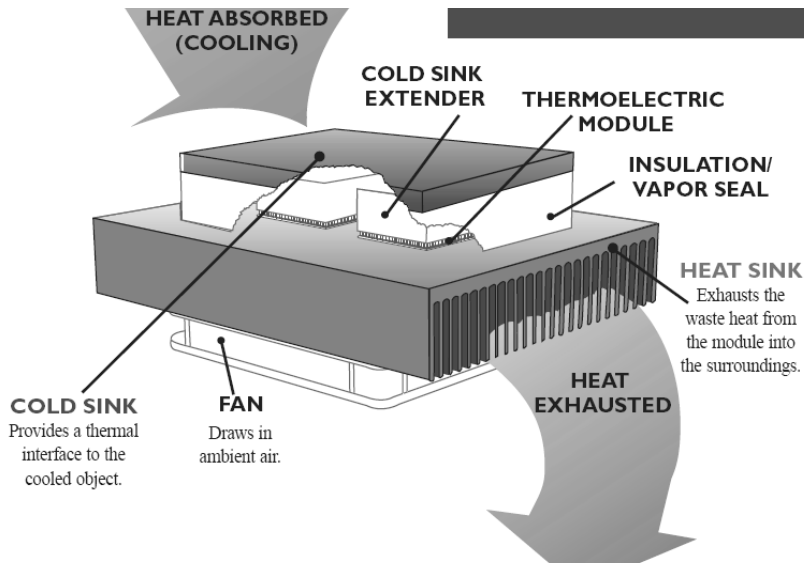


Figure 27 - Typical Thermo-electric Cooling Assembly²⁸

After careful evaluation of our temperature regulation options, the cold plate, and re-circulating chiller or the thermoelectric cooling system, the thermoelectric cooling system was chosen as the primary option to pursue. Cost analysis of both options was done in addition to examining size, weight and overall efficiency of the cooling systems. The thermoelectric cooling system proved to excel in all comparisons conducted.

There are many advantages when considering the use of a thermoelectric cooling assembly over a compressor. Thermoelectric modules have no moving parts and do not require the use of chlorofluorocarbons. The only moving part on a thermoelectric assembly is a fan that is tested and engineered to be virtually vibration and noise free. Therefore, TEC devices are incredibly reliable and virtually maintenance free. TEC

assemblies may be mounted in orientation and still function properly, which is a key element when considering our design application. Another significant advantage to TE module cooling is the relative size when compared to a cooling system requiring a compressor. The compact size of a TE assembly makes them ideal for applications that are size or weight limited where even the smallest compressor would not suffice. Using TE modules allows for operation in applications where precise heating and cooling are necessary.

TE Technology, Inc. is one of the leading providers for thermoelectric cooling assemblies. “With over 40 years of experience in thermoelectric product design, prototyping and manufacturing, TE Technology has the experience and knowledge to deliver thermoelectric cooling solutions for all businesses, both large and small. TE Technology offers the highest quality thermoelectric coolers for all of your cooling needs. We design and manufacture thermoelectric cold plates, liquid coolers, and thermoelectric coolers for thermoelectric cooling applications that demand extremely high reliability”²⁹. TE technology has standard cold plate assemblies which contain a cold plate to be placed in contact with the aluminum mounting plate of the pressure vessel. Attached to the other side are thermoelectric modules and a heat sink to complete the assembly. With the use of multiple CP-218 cold plate assemblies we should be able to obtain sufficient cooling for our application.

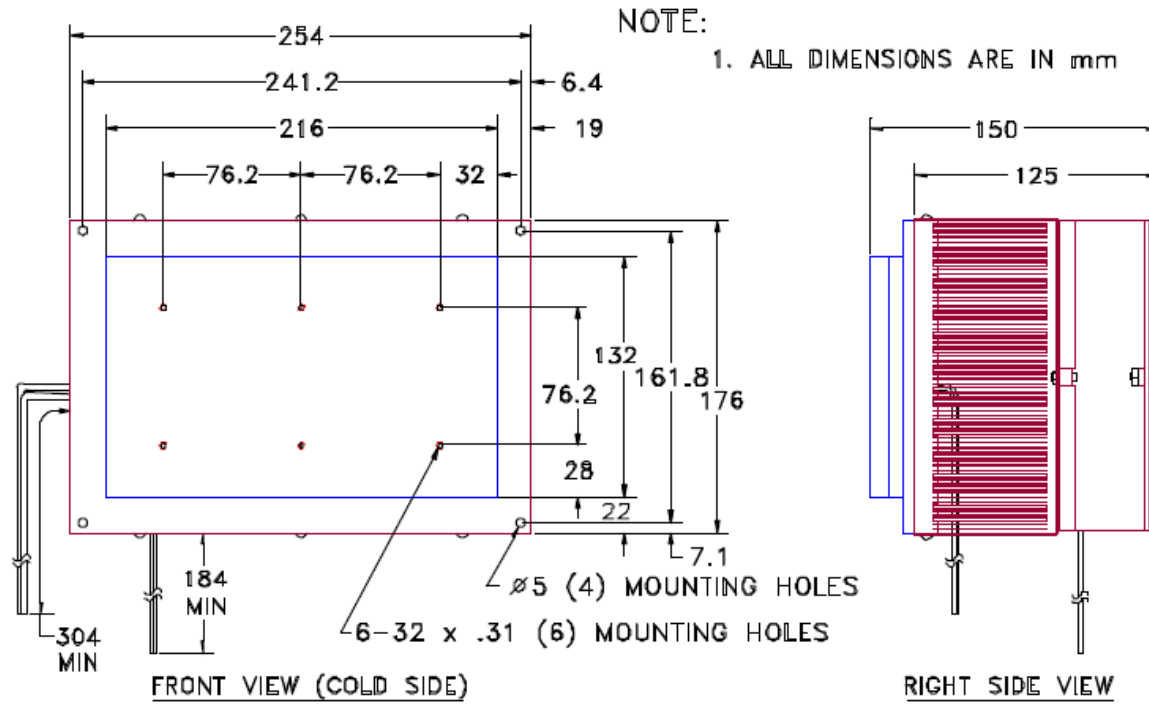
VI - D - 1 Cooling Assembly

The CP-218 (Figure 28) is able to handle heat load up to 218 Watts at a 0 degree temperature difference. The MicroMAPS system generates a maximum of 27 watts while booting up. For our operating conditions, the cold plate assembly has the capability of

cooling to -50 deg C below ambient. The cargo bay environment will stabilize to 10 deg C, so the maximum temperature difference required will be 30 deg C. The CP-218 uses six thermoelectric modules in conjunction with a high efficiency bonded-fin heat sink in order to keep the system small yet effective. In order to compensate for the possible extreme temperatures the Altair cargo bay may experience while stationary on the runway, we recommend the use of two CP-218 cooling assemblies run simultaneously³⁰.



Figure 28 - Thermoelectric Cooling Assembly, CP-218³¹



VI - D - 2 Temperature Regulator

Each cold plate assembly may be used in conjunction with TE Technology's TC-24-25 RS232 temperature controller. The TC-24-25 RS232 is a bi-directional controller for thermoelectric assemblies. The "H" bridge configuration of the solid state MOSFET output devices allows the bi-directional flow of current through the thermoelectric modules. This allows the thermoelectric assembly to both heat and cool. Highly efficient N-channel output devices are used for this control mode. This controller may be programmed via an RS232 communication port for direct interface with a compatible PC. Once the desired parameters are established, the PC may be removed from the loop and the TC-24-25 RS232 becomes a stand alone controller. This controller is capable of operating from an input supply voltage of 12 through 28 VDC. Its self-contained MOSFET output devices are able to deliver load currents from 0.1 to 25 amperes. With

this unit, temperature may be controlled precisely with a resolution and accuracy of 0.05 deg.³³

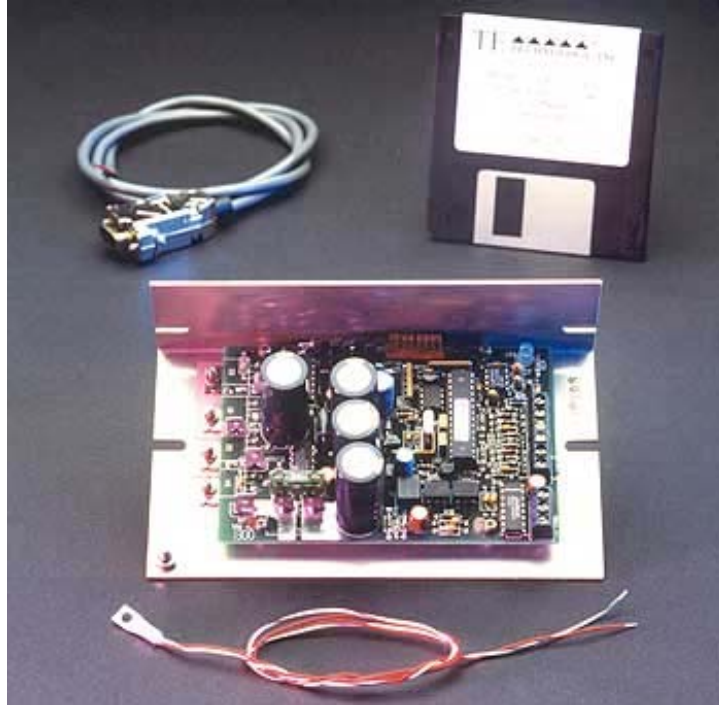


Figure 30 - TC-24-25-RS232 Temperature Controller³⁴

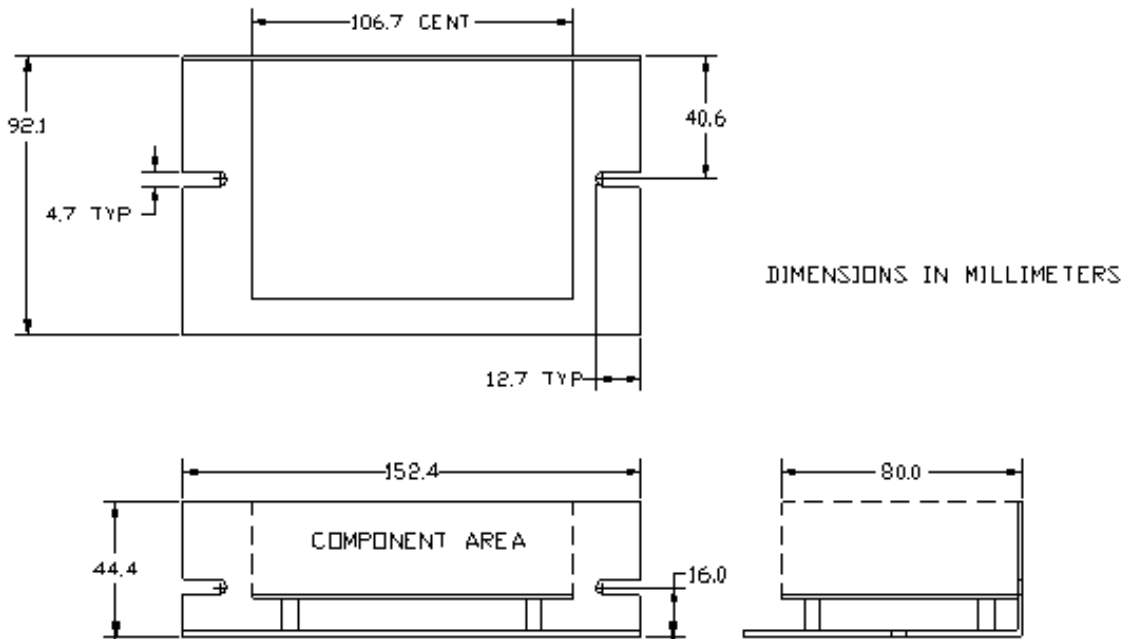


Figure 31 - Dimensioned TC-24-25-RS232 Temperature Controller³⁵

Table 7 - Controller Specifications³⁶

<p> Input voltage from 12 to 28 VDC Self-contained, 0.1 to 25 A load rating PC programmable via RS232 communications port Bi-directional control for heating and cooling applications Solid state "H" bridge operation Control temperature of -20°C to 100°C Proportional (P), Integral (I) and Derivative (D) control that can be selected as P, PI, PD or PID; or on/off with an adjustable hysteresis Temperature resolution of 0.05°C Pulse width modulation of output Selectable modulation frequency of 675 Hz or 2700 Hz Control stability of $\pm 0.05^\circ\text{C}$ 1500 VAC isolated RS232 communications interface Controls up to 680 W Set temperature selectable PC set with controller stand alone operation Remote user set temperature potentiometer 4 to 20 MA current loop 0V to 5V adjustable range Differential temperature control No computer programming experience required to use the communications software program Command set is provided so programmers may create their own software interface or embedded controller applications PC configurable alarms for 5VDC at 25MA Alarm cancel: selectable via PC or remote contacts Non-volatile memory retention of parameters Power Supply </p>
--

The power supplies offered by TE Technologies are AC/DC fixed voltage units. This type of power supply will not function in the Altair, because the Altair has direct DC power outlets. For our application, a universal DC/DC converter must be utilized to channel and regulate the Altair's existing power supply. After extensive research, the company ASTRODYNE was found to provide the cheapest solution to our power specifications. ASTRODYNE currently offer the SD-350 series 350 watt single output DC/DC converter. The SD-350B will supply 24 VDC as required by the CP-218 coolers.

This unit may accept a DC voltage ranging from 18-36 V, which falls within the Altair's DC voltage supplied of 28-32 V. Other specifications can be viewed in Figure 34.³⁷



Figure 32 - Astrodyne SD-350 Series 350 Watt single output DC/DC converter³⁸

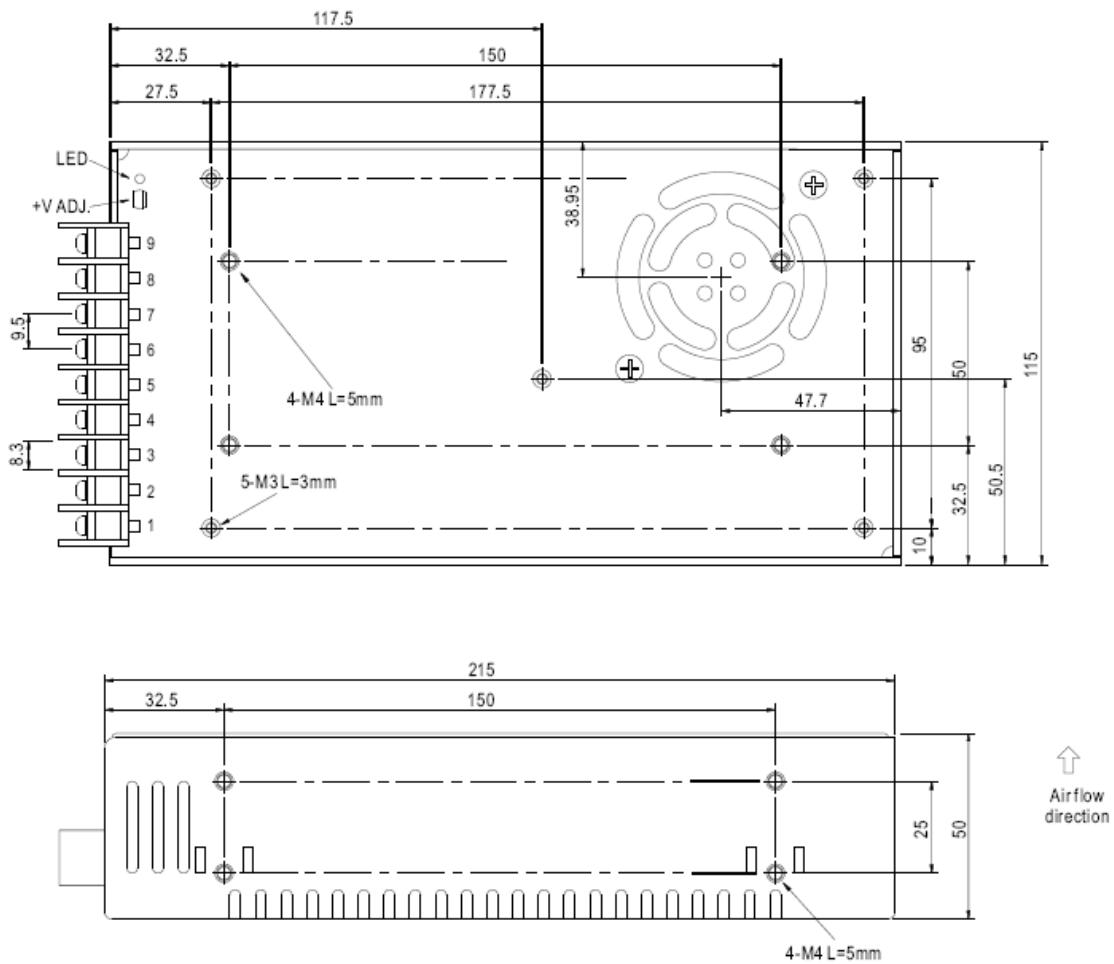


Figure 33 - Schematic of the Astrodyne SD-350 Series single output DC/DC converter³⁹

MODEL		SD-350B			
OUTPUT	DC VOLTAGE	5V	12V	24V	48V
	RATED CURRENT	57A	27.5A	14.6A	7.3A
	CURRENT RANGE	0 ~ 57A	0 ~ 27.5A	0 ~ 14.6A	0 ~ 7.3A
	RATED POWER	285W	330W	350.4W	350.4W
	RIPPLE & NOISE (max.) Note.2	100mVp-p	120mVp-p	150mVp-p	200mVp-p
	VOLTAGE ADJ. RANGE	4.5 ~ 5.5VDC	11 ~ 16VDC	23 ~ 30VDC	43 ~ 53VDC
	VOLTAGE TOLERANCE Note.3	±2.0%	±1.0%	±1.0%	±1.0%
	LINE REGULATION	±0.5%	±0.3%	±0.2%	±0.2%
	LOAD REGULATION	±1.0%	±1.0%	±1.0%	±1.0%
INPUT	SETUP, RISE TIME	300ms, 50ms at full load			
	EFFICIENCY (Typ.)	74%	80%	80%	84%
	DC CURRENT	18A/24V	20A/24V	22A/24V	22A/24V
PROTECTION	INRUSH CURRENT (max.)	C:50A/48VDC D:50A/96VDC			
	OVER LOAD	105 ~ 135% rated output power Protection type : Shut down o/p voltage, re-power on to recover			
	OVER VOLTAGE	5.75 ~ 6.75V	16.8 ~ 20V	31.5 ~ 37.5V	53 ~ 65V Protection type : Shut down o/p voltage, re-power on to recover
ENVIRONMENT	OVER TEMPERATURE	95°C±5°C (TSW1) Detect on main power transistor Protection type : Shut down o/p voltage, recovers automatically after temperature goes down			
	WORKING TEMP.	-20 ~ +60°C (Refer to output load derating curve)			
	WORKING HUMIDITY	20 ~ 90% RH non-condensing			
	STORAGE TEMP., HUMIDITY	-40 ~ +85°C, 10 ~ 95% RH			
	TEMP. COEFFICIENT	±0.03%/°C (0 ~ 50°C)			
SAFETY & EMC (Note 4)	VIBRATION	10 ~ 500Hz, 2G 10min./1cycle, 60min. each along X, Y, Z axes			
	SAFETY STANDARDS	24V and 48V input design refer to LVD			
	WITHSTAND VOLTAGE	I/P-O/P:1.5KVAC I/P-FG:1.5KVAC O/P-FG:0.5KVAC			
	ISOLATION RESISTANCE	I/P-O/P, I/P-FG, O/P-FG:100M Ohms/500VDC			
	EMI CONDUCTION & RADIATION	Compliance to EN55022 (CISPR22) Class B			
OTHERS	EMS IMMUNITY	Compliance to EN61000-4-2,3,4,6,8; ENV50204 heavy industry level, criteria A			
	MTBF	209.4K hrs min. MIL-HDBK-217F (25°C)			
	DIMENSION	215*115*50mm (L*W*H)			
	PACKING	1.1Kg; 12pcs/14.4Kg/0.98CUFT			

Figure 34 - Specifications of the Astrodyne SD-350 Series single output DC/Dc converter⁴⁰

VI - D - 3 Thermoelectric cooling system solution

After running several simulations with CFDesign, using different types of coolers, it appears that using only one 218 W cooler is insufficient. The results obtained from these simulations show that the variation of temperature is far too slow and does not meet our expectations.

When using a two 218 W cooler system, the results from the simulation finally met our requirements. The following figure shows MicroMAPS temperature versus time.

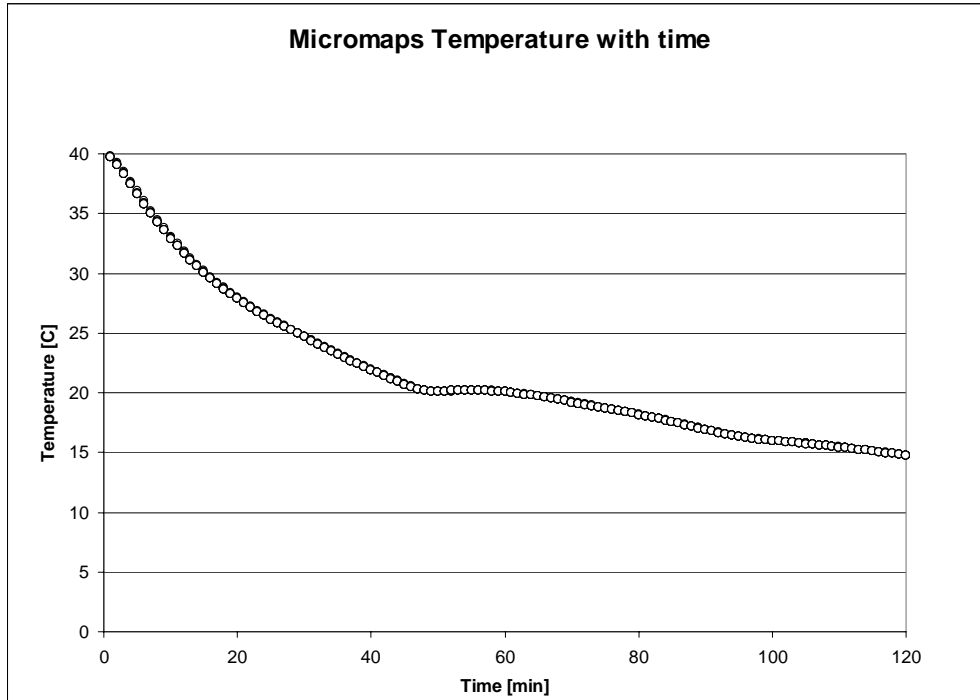


Figure 35 - Temperature variation with two 218 Watt coolers

With the initial temperatures of the pressure vessel and the payload bay set to 40°C, it appears that after the first 30 min, just before take off, the temperature of the MicroMAPS is 25 °C. 45 minutes after take off, the temperature attained is 19 °C.

This figure illustrates the fact that the cooling system is capable to decrease the temperature of MicroMAPS to approximately 15°C in 90 minutes under the worst conditions.

However, since the cooling system will require 90 minutes to cool down, the MicroMAPS will be able to start the data acquisition only 90 minutes after the start of the mission or Altair's take off. The following graph shows a simulation where the cooling process starts 30 minutes prior to Altair's take off.

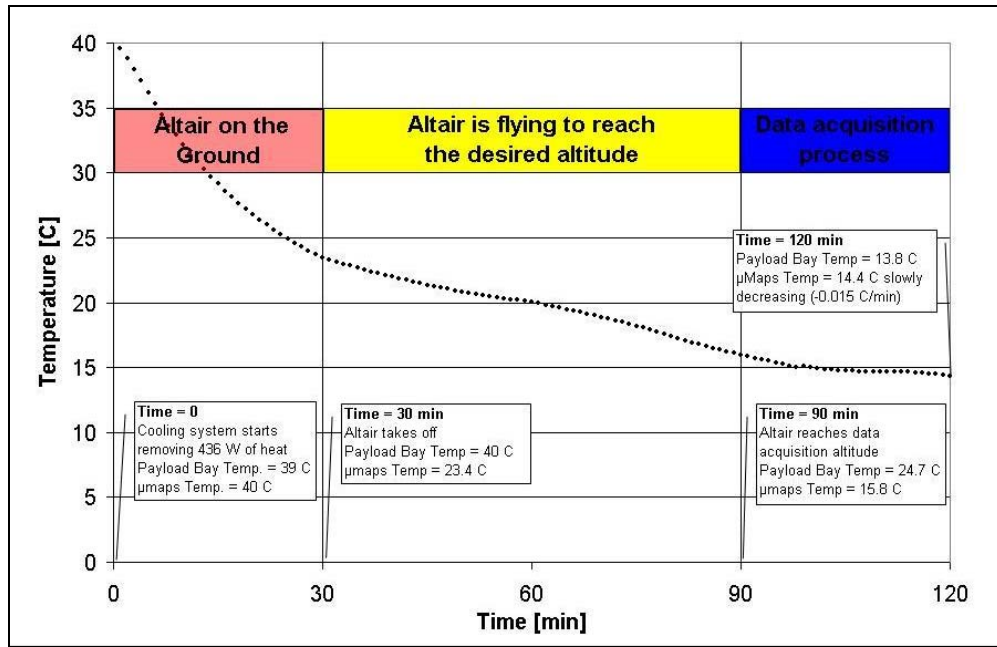


Figure 36 - MicroMAPS Instrument Temperature Variation during flight (simulation)

As illustrated it will be possible to begin the data acquisition process 60 minutes after take off with the conditions described (worst scenario).

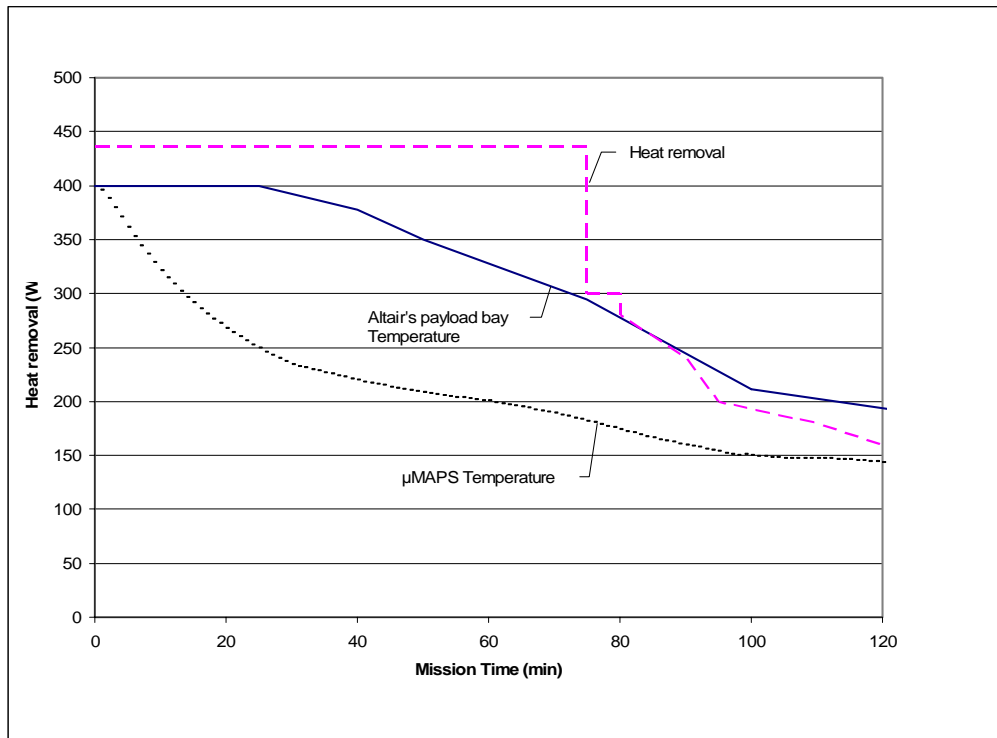


Figure 37 - Heat removal required and corresponding temperature versus time

By using the thermal control system and varying the heat removal load for each of the coolers as shown in the previous figure, it is possible to keep the temperature stable. In fact, the temperature slowly converges to the final temperature. The temperature decreasing rate obtained in this simulation is lower than the one obtained when no cooling system was used. In other words, the temperature of MicroMAPS is more stable because the variation rate is lower than the rate obtained by only natural convection. This fact is illustrated in the following figure. The temperature varies at a rate lower than 0.05 °C per minute after 100 minutes, while it is larger than 0.2 °C per minute at the same time using natural convection.

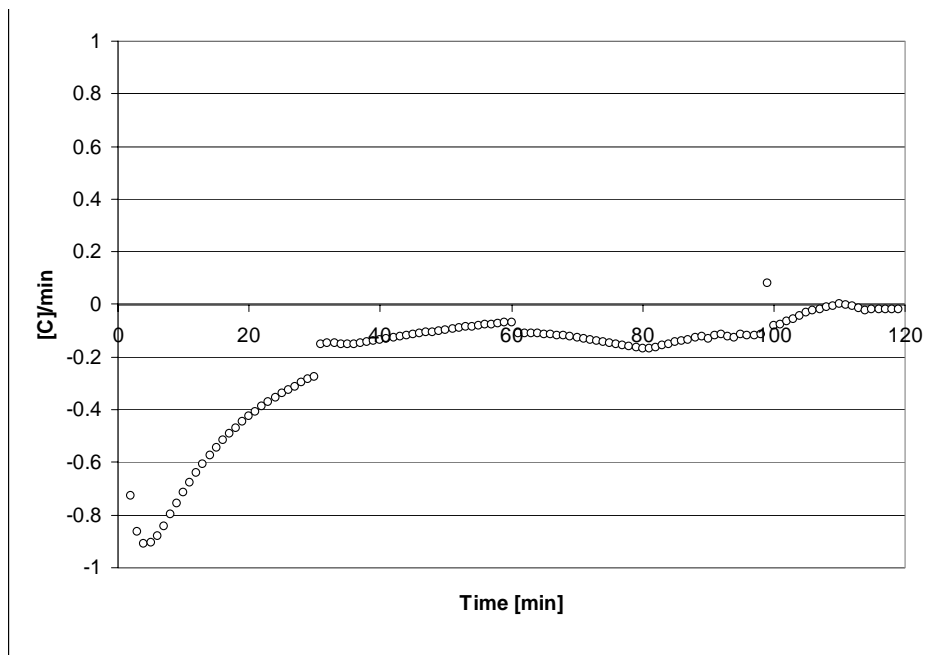


Figure 38 - Rate of Temperature Variation versus time

As noted before, these results describe the variation of the temperature in the case where maximum temperature is assumed. If we assume that the system will be mostly used under standard atmospheric condition where the ambient sea level temperature is approximately 15 °C, the initial temperature of all the components inside and outside the

pressure vessel can also be assumed to 15 °C. Using this assumption and the Altair's payload bay temperature assumption during flight as described previously, the temperature distribution and variation with time would be completely different, as shown by the following figure.

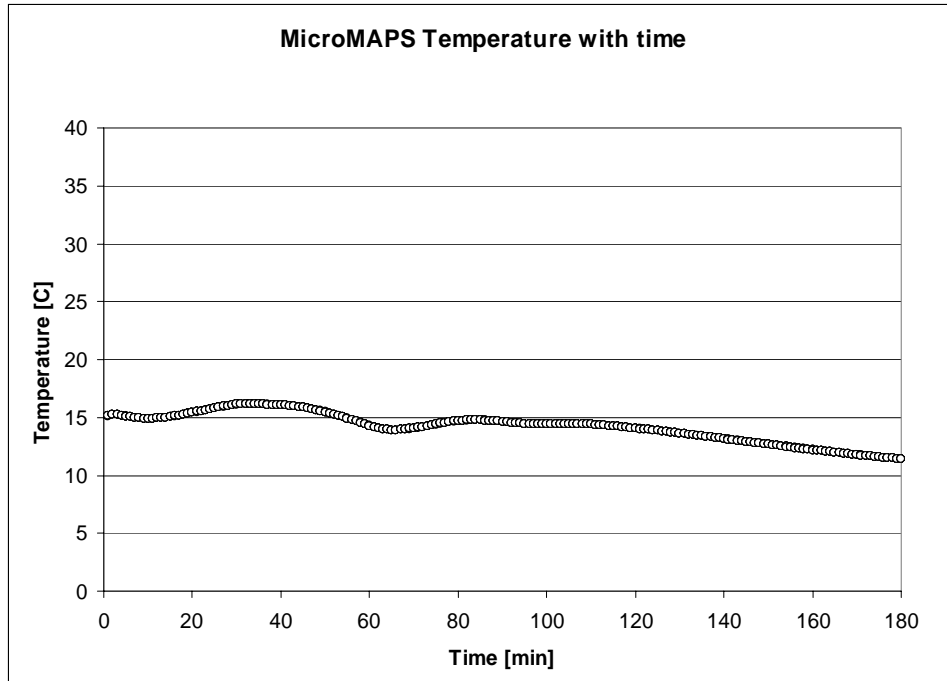


Figure 39 - Temperature variation of MicroMAPS for an initial system temperature of 15°C

In this case the cooling system is not used to decrease the global temperature of the pressure vessel but rather to maintain the initial temperature. The heat removed by the coolers cancels the heat gain by the system through conduction with the higher temperature of the payload bay. In such situation, it is obvious that the data acquisition process could be done much sooner.

VI - D - 4 Thermal distribution of the Aluminum plate

The following figures illustrate the temperature versus the time of the aluminum plate and the effect of the cooling process.

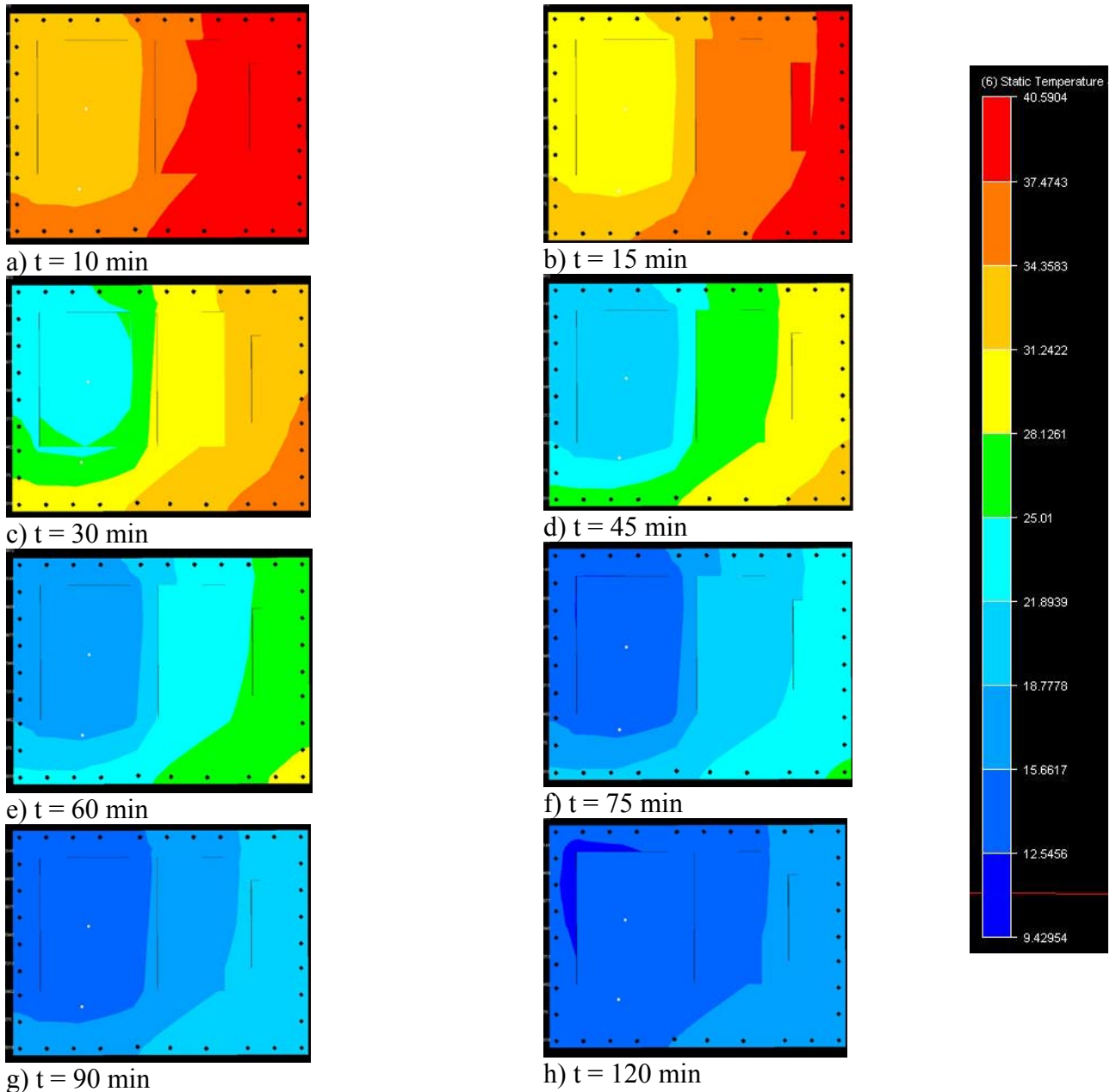


Figure 40 - Base plate temperature with time and heat propagation during cooling process.

VI - D - 5 Configuration

The two CP-218 coolers will be mounted directly to the aluminum plate on the exterior of the pressure vessel. There are four tapped holes in each cold plate so that the assembly may easily be attached to the aluminum mounting plate. The SD-350B DC/DC converted will be connected to the Altair's power supply. The converter and the TC-24-25-RS232 temperature controller will be connected in series with the CP-218 cooling assembly. Both the converter and the temperature controller will be mounted close to the pressure vessel onto the walls of the payload bay.

VII Data Acquisition System and Power Supply System

The objective of the data acquisition and power supply systems is to provide stable power and data collection methods to and from the payload. The payload consumes 24 Watts on average (50 Watts peak) and requires three signals, +5V and -15V and +15V. The computer requires less than 10 Watts. The payload data connection utilizes an RS-422 standardized connector. Two methods are available for data collection. The onboard data acquisition system in the Altair can be used. This built-in system is not necessary if the current data acquisition system is used. The aircraft will require power on the ground prior to take off. The cold plate power must be initialized before takeoff to prevent overheating and provide early stabilization of the payload.

The current data acquisition solution, as was deployed on the Proteus, is independent of the aircraft systems and relies on the pilot powering up the computer at the appropriate time. This custom built computer controls the payload and collects data in-flight. This data may be downloaded from the computer upon landing, through a physical Ethernet connection. This does not allow for real time data collection. In addition, since this is a UAV, there is no pilot to initialize the equipment, so an automatic timer must be used to start the MicroMAPS instrument and data collection equipment.

The Altair's on board data acquisition equipment provides an ideal way to control the payload. There are two inherent advantages in this system. The advantages are independency from the pilot and real time data collection. These both alleviate the previous problem of relying on the pilot to initialize and shut down the payload systems

and allow for real time verification and analysis of the data. Payload control is then given to the payload owner, on the ground, through a redundant control system.

VII - A Payload Data Acquisition Rate

The payload produces less than 0.5 MB of information per day in a 100% on condition. The in-flight data transfer rates for the Altair exceeds this.

VII - B Current Setup/Independent Method

The current payload setup uses the following equipment. Of these items, only the fuses, the EMI filter, and a modified DC-DC power converter would be required if the Altair's data collection system were used.³²

Two 5 amp fuses in parallel connected to an Electromagnetic (EMI) filter transmit power to a DC-DC converter. This power converter, a Martek Power type NB50S, supplies power to internal payload sensors, the MicroMAPS instrument and the computer power supply. This main power converter accepts 14 to 40 volts, making it compatible with many platforms, including the Altair. A Tri-M Systems Engineering CPU board, type MZ104+ ZFx86, communicates directly with the instrument and the internal payload sensors. Data is retrieved upon landing through an Ethernet connection. We recommend a GPS board if the Altair is not used for data collection, connected to the PC104. This GPS board may be connected directly to the current CPU board and would require an external antenna.³²

VII - C Altair Data Collection

VII - C - 1 Overview

The Altair is capable of either a C-band Line-Of-Sight (LOS) communication or Ku-band Over-The- the Horizon (OTH) Satellite Communication (SATCOM). The General Atomics –Aeronautical Systems, Inc. (GA-ASI) Ground Control Station (GCS) incorporates workstations that allow scientists to record and exploit down-linked payload data in real time. The MicroMAPS data connection is compatible with the standard payload connector currently employed on the Altair.²

VII - C - 2 Concept of Operation

Deployment of the Altair involves an aircraft with a Ground Control Station (GCS) and the necessary support personnel and equipment. The operators of the payload can utilize the General Atomics GCS or their own payload control workstations in a trailer of their own design. Figure 37 shows a typical Altair deployment.²

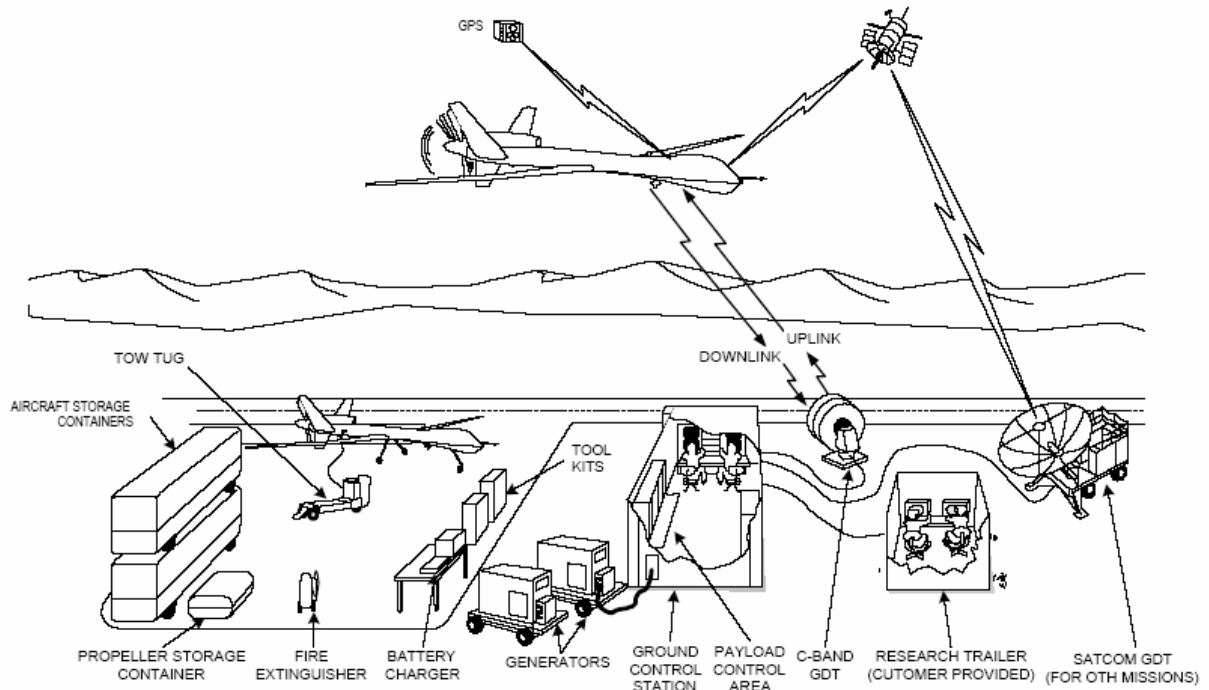


Figure 41 - Altair Deployment

VII - D Payload Bay Characteristics

The payload weight, volume, and power characteristics are given in table 5.

Neither the weight, volume, nor the power available will act as limiters of the proposed setup.

Parameter	U.S. Measurement	Metric
Overall Payload with Max Fuel	660 lb	299 kg
Internal Payload Volume Capacity	55 Cubic Feet	1557 liters
Internal Payload Weight Capacity	750 lb	39 kg
Inboard Wing Station	500 lb	227 kg
Middle Wing Station	350 lb	159 kg
Outboard Wing Station	None	None
C-band LOS Range Limit	100 NM	
Power Dissipation (through ducting)	1250 Watts	
Humidity	Up to 100% condensing	
Shock	10g for 11 seconds	
Vibration	2g peak at 100Hz	

Power Available	28 to 30 VDC, 4.5 kW at 50000 ft
-----------------	----------------------------------

Figure 42 - Altair Payload Bay Characteristics

VII - E Data Acquisition with the Altair

The MicroMAPS sensor has a single serial port used for communication. It uses the RS 422 serial standard with XMODEM protocol. This is a simple file transfer method that allows for data blocks of 128 bytes. The XMODEM protocol uses a one byte checksum to validate data blocks and requires acknowledgement of every single block transmitted. The data collection sequence is as follows. The computer will send a signal initiating data collection upon which the MicroMAPS instrument will collect and transmit the data. The computer is required to acknowledge the receipt of the data. A slight modification of the MicroMAPS internal software may be required to send the correct data packet size (128 bytes instead of 8 bytes). Further research may find this unnecessary. The Altair will provide flight information such as GPS location, speed, altitude and time of flight directly to the GCS workstation.

VII - E - 1 Electrical Power

The aircraft provides power from two engine driven generator units. A fixed 28 to 30 VDC and 4.5kW measured at the output of the power source is available to the internal payload bay.

VII - E - 2 Electromagnetic Compatibility

The payload must be able to withstand a radiated Electromagnetic Interference (EMI) environment created by aircraft systems as defined in MIL-STD-461, CS101, and RE102. The aircraft produces the following additional RF emissions: C-band

datalink (4.4 to 5 GHz), FAA Transponder (1100 MHz), GPS unit (1.575 GHz, Ku-band datalink 11.45 to 14.5 GHz).

VII - E - 3 Payload Interface Cables

The following aircraft interface cables are available through the internal payload bay:

- RCM data interface cable RS-422 bus with RCM for control and status)
- Power interface cable (28 VDC)
- SPMA data interface cable (high-bandwidth digital data to SPMA)
- Analog video cable (RS-170, if required)

Figure 39 shows the interface cables necessary to connect payloads with various interface requirements. The MicroMAPS Equipment utilizes a RS-422 connector. A standard generic payload interface connector may allow the utilization of the RS-422 connection instead of building an independent data acquisition system. The proposed setup would use the circled connection.

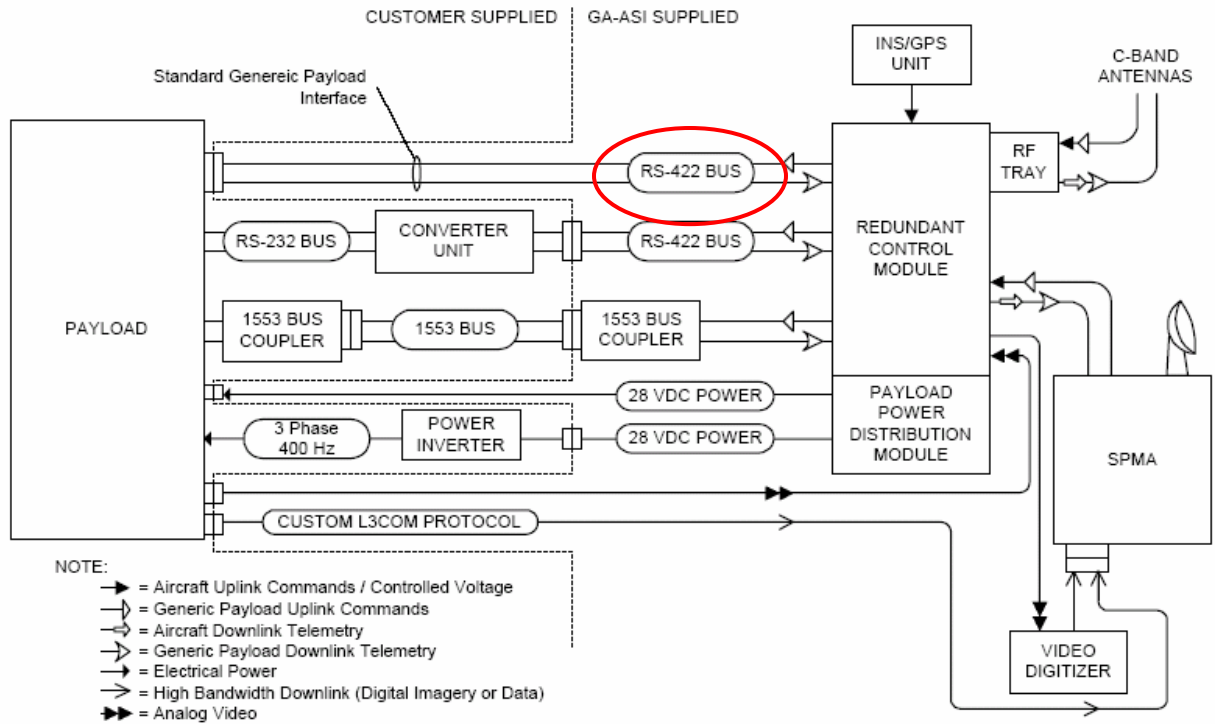


Figure 43 - Payload Data Cable Interface

VII - E - 4 Power Interface Cable

A 19 pin circular power connector with a flange provides power to the payload bay. There is a maximum of 23 amperes per pin or 3.8 kW.

VIII Weight and Cost Analysis

Table 9 shows a break down of the cost of the individual parts of the MicroMAPS Package. This table shows an approximate price for completion of this project assuming that the computer and power supply currently in use will be reused. The prices for materials, manufacturing, and miscellaneous are approximate. The costs associated with operating the UAV are not included in this table.

Table 8 - Cost Breakdown

Component	Quantity	Price
TE Technology CP-218 Cooling Assembly	2	\$563
TE Technology TC-24-25-RS232 Temperature Controller	2	\$481
ASTRODYNE SD-350B DC/DC Converter	2	\$129
Materials (aluminum 2014)	~40 lbs	\$2 /lbs
Manufacturing	30 hrs	\$60 /hr
Miscellaneous (bolts, connectors, valves, and etc.)		\$500
Total		~\$4800

IX Appendix

IX - A *Different Cooling Systems*

IX - A - 1 **Heatsinks**

A heatsink is simply a metal surface with pins or fins rising up off the surface.

Heatsinks are made to expand the surface area, which increases the amount of heat that can be cooled by the ambient air. Each heatsink thermal solution can be categorized into five different types of solutions:

- **Plate Fin:** These come in a wide variety of sizes, and the tooling costs depend on the distance between the fins. The smaller the distance the better is the thermal performance.
- **Round Pin:** These come either in a staggered or a straight-line array. They are best suited for applications in which the direction of airflow is uncertain, where air pressure drop is not a concern.
- **Elliptical Pin:** The performance is less than round pin heatsinks but better than plate fin heatsinks. They are designed for specific airflow problems and have a great pressure drop capability. Their specific design lets air pass through the heatsink and cool other components.
- **Custom Cast Enclosures:** This is an enclosure for an electronic device that also incorporates a heatsink. They are made specifically for devices that need to be enclosed as well as cooled.
- **Fan Heatsink:** Almost all heatsinks can have a fan attached. The fan blows air across the fins/pins to cool them. This provides a significant increase in cooling capacity and better thermal performance.¹⁶

The most simple is the passive heatsink solution, which is used in applications that can either provide natural convection or that does not require much airflow. These types of solutions can normally handle a load of about 5-25 watts. The next level up is the semi-active heatsink solution, which gets extra airflow from system fans. These can usually handle a load of about 15-50 watts. Active heatsink solutions actually incorporate a fan, which is attached to the solution. They can handle a load of about 10-160 watts. The fifth type of solution is the phase-change recirculating system. This solution involves heatpipes that either contain a wick or are helped by gravity. This solution can handle a load of about 100-150 watts.

The performance indicator of heatsinks is thermal resistance (q), which is measured in $^{\circ}\text{C}/\text{W}$. For a heatsink with a thermal resistance of $q = 2^{\circ}\text{C}/\text{W}$, every watt of heat dissipated increases the temperature by 2°C . The larger the heatsink, the more surface area it has and the better the thermal resistance. A rough formula for calculating the area needed for a heatsink is:

$$A = \left(\frac{50}{\Theta} \right)^2$$

Where the area is in cm^2 and q is in $^{\circ}\text{C}/\text{W}$.

IX - A - 2 Fans

Fans can be used in passive thermal solutions to blow hot air off of heatsinks, or they can be used alone to ventilate cool intake air across the integrated circuit component, pushing warm air out. There are some side effects that come from using fans. One issue is dust buildup, which affects the performance of the fan. Dust will slow down the fan's airflow, causing a higher chance of failure. Other side effects include acoustic noise,

vibration, and power consumption. Increased noise and high mechanical vibrations can be prejudicial to the accuracy of the data acquired.

IX - A - 3 Heat pipes

Heatpipes are mostly used in combination with other products but may also be used alone. A heatpipe is basically a sealed pipe, filled with liquid, with a wick structure inside. One end is called the evaporator and the other is called the condenser. When heat is applied to any part of the heatpipe the liquid will boil in the evaporator end. With this increase in vapor pressure, the evaporated liquid will flow towards the condenser end where it is cooler. The vapor is then condensed back to its liquid form and flows back to the evaporator end. Many different liquids can be used as the working fluids like helium, nitrogen, water, acetone, ammonia and methanol. The choice of the working fluid is made according to the operating temperature of the system.¹⁶

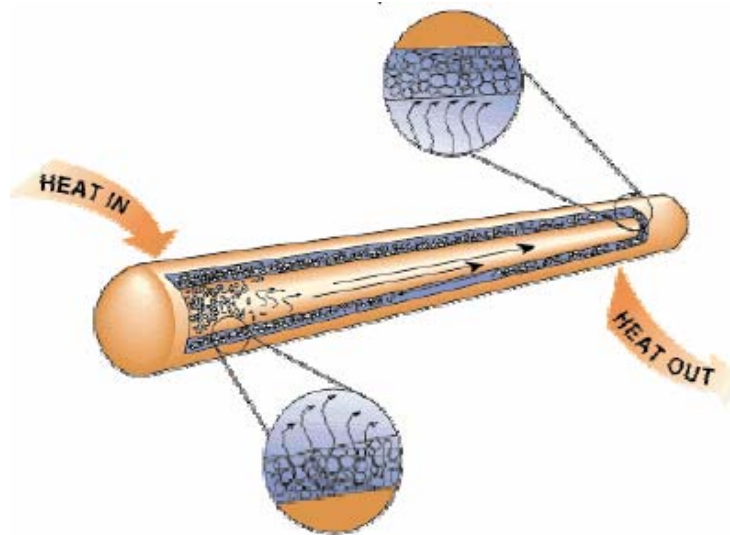


Figure 44 - Description of the functioning of a heat pipe.

IX - A - 4 Liquid Cooling

Liquid cooling is essentially a radiator for the system. Just like a radiator for a car, a liquid cooling system circulates a liquid through a heatsink. As the liquid passes through the heatsink, heat is transferred from the system to the cooler liquid.⁷

The hot liquid then moves out to a radiator at the back of the case and transfers the heat to the ambient air outside of the case. The cooled liquid then travels back to the system to continue the process.

Electronic components are mounted on cold plates or heatsinks (fin stock) to transfer heat to the coolant. One or more pumps are used to circulate the flow through the system and a liquid reservoir is used to maintain the system pressure and compensate for any small leakage that may occur.

A cold plate consists of a metal plate with coolant circulating through the passages embedded within it. The flow distribution within these passages should result in a uniform cooling over the entire surface of the cold plate. Similarly, the fin thickness and fin spacing of a heat sink need to be chosen appropriately for obtaining the desired flow rate and heat transfer performance. Two main types of cold plates are used in practical applications:

- Tubed flow cold plates

A copper or a stainless steel tube is pressed into a channeled aluminum extrusion (see Figure 40). The performance of the cold plate improves as the number of passes increase

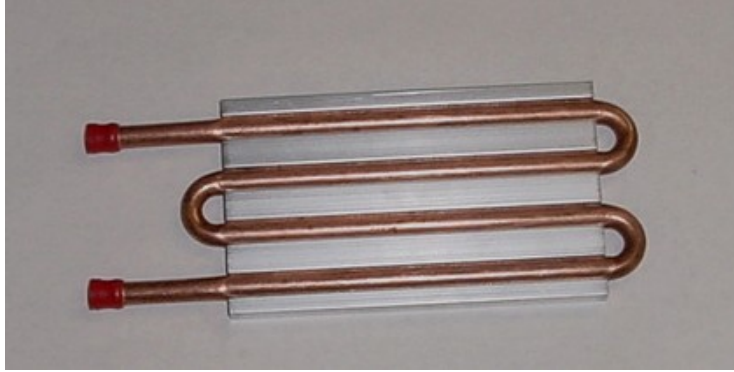


Figure 45 -Photograph of a tubed flow cold plate manufactured by Lytron ⁴¹.

- Distributed flow cold plate

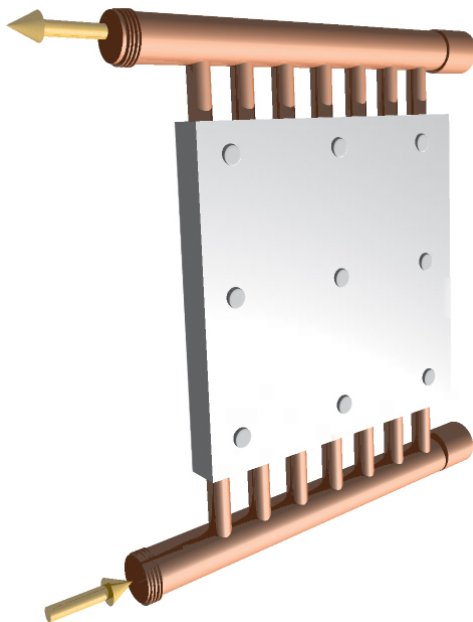


Figure 46 -Representation of a distributed flow cold plate.

As shown in Figure 41 the liquid flow is distributed within the cold plate. Cross-flow tubes are embedded within the solid block of the cold plate.¹⁶

Liquid cooling has conventionally been used for thermal management of electronics in defense, power, medical laser, and diagnostic equipment. It is now being increasingly used for the cooling of high-end servers, telecommunication equipment.

Liquid cooling offers several advantages as a removal mechanism in applications where power densities exceed the limits of air-cooling and results in a compact design.

The other benefit of liquid cooling is the reduction of noise within the system. Most current heatsink and fan combinations tend to generate a lot of noise from the fans that need to circulate air over the system. Generally there are two moving parts to a liquid cooling system. The first is the impeller which is a fan immersed in the liquid to circulate the liquid through the system. These are generally fairly low in noise because the liquid acts as a noise insulator. The second is a fan at the exterior of the case to help pull air over the cooling tubes of the radiator. Both of these do not need to run at very high speed, which reduces the amount of noise by the system.

Design of a liquid-cooling system requires sizing of individual components so that the desired flow is delivered to the cold plates and heatsinks on which the electronics components are mounted. The individual cold plates and heatsinks also need to be designed so as to achieve effective and uniform cooling over the entire surface.

References

- 1 "Altair Experimenter's Handbook". General Atomics Aeronautical Systems Inc. October 2001. San Diego, Ca.
- 2 Resonance Ltd Online. "MicroMAPS-A Low-Cost Nadir-Viewing Remote Sensor For the Detection of CO and N2O in the Troposphere." Oct. 2004. November 2004. URL: <<http://www.resonance.on.ca/mmmaps.html>>. [cited December 7th, 2004]
- 3 Perseus B Payload User's Guide" Aurora Flight Sciences Corporation, 2004
- 4 Global Aircraft, Helios, URL: <http://www.globalaircraft.org/planes/helios.pl> [Cited Dec 8th 2004]
- 5 Air-Attack.com, Helios Solar Powered UAV, <http://www.air-attack.com/page.php?pid=17> [Cited Dec 8th 2004]
- 6 "Remotely Operated Aircraft Systems" General Atomics Aeronautical Systems Inc. URL: <http://www.uav.com> [Cited Dec. 8th 2004]
- 7 Office of the Secretary of Defense, March 11, 2003. UAV roadmap URL: www.acq.osd.mil/usd/uav_roadmap.pdf [cited December 7th, 2004]
- 8 See reference 7
- 9 See reference 7
- 10 See reference 7
- 11 See reference 1
- 12 See reference 1
- 13 See reference 1
- 14 Sargent Fletcher Inc. Homepage URL: <http://www.sargentfletcher.com/spp.htm> [cited December 7th, 2004]
- 15 Butler, M. C., and Loney, T. "Design, Development and Testing of a Recovery System for the Predator™ UAV" 13th AIAA Aerodynamic Decelerator Systems Technology Conference URL: <http://www.butlerparachutes.com/PDF/AIAA95.pdf> [cited December 7th, 2004...]
- 16 Beer, Ferdinand P.; Johnston, E. Russell; DeWolf, John T. "Mechanics of Materials: Third Edition". McGraw-Hill Higher Education. New York, NY. 2002
- 17 Davenport, William; Kapania, Rakesh. "Beam Under Transverse Loads".
- 18 See reference 17
- 19 Hybrid Connectors, Fischer Company, URL: <http://www.fischerconnectors.com/catalog/hybrid-brochure.pdf> [cited December 7th, 2004]
- 20 SMC Corporation of America Homepage URL: <http://www.smcusa.com/sections/products/valves.asp> [cited December 9th, 2004]
- 21 The Valve Shop, www.thevalveshop.com
- 22 (<http://www.unitedseal.com/>)
- 23 (<http://www.aerorubber.com/>)
- 24 See reference 1
- 25 Heat transfer in electronic equipment, American Society of Mechanical Engineers, 1983
- 26 Physical Properties of Aluminum Alloys. January 2005 URL: <http://www.thermaflo.com/engref_physical.shtml>
- 27 Heat transfer. J.P. Holman. New York : McGraw-Hill, c1997 8th ed
- 28 TE Technoly, Inc Homepage. March 2005. URL:< <http://www.tetech.com/>>. [Cited April 2005]
- 29 See reference 28
- 30 See reference 28
- 31 See reference 28
- 32 See reference 28
- 33 See reference 28
- 34 See reference 28
- 35 See reference 28
- 36 See reference 28
- 37 "High Performance DC/DC", Astrodyne Homepage. 2004. URL:< http://www.astrodyne.com/astro/dept_dcde.asp?dept%5Fid=6>.

[Cited April 2005]

38 See reference 37

39 See reference 37

40 See reference 37

41 Lytron Homepage. 2002-2004. November 2004. URL: <<http://www.lytron.com/>> [cited December 7th, 2004]